Coverage Analysis and Scaling Laws in Ultra-Dense Networks

Imène Trigui, *Member, IEEE*, Sofiène Affes, *Senior Member, IEEE*, Marco Di Renzo, *Fellow, IEEE*, and Dushantha Nalin K. Jayakody, *Senior Member, IEEE*

***Abstract*— In this paper, we develop an innovative approach to quantitatively characterize the performance of ultra-dense wireless networks in a plethora of propagation environments. The proposed framework has the potential of simplifying the cumbersome procedure of analyzing the coverage probability and allowing the unification of single- and multi-antenna networks through compact analytical representations. By harnessing this key feature, we develop a novel statistical machinery to study the scaling laws of wireless networks densification considering general channel power distributions including small-scale fading and shadowing as well as associated beamforming and array gains due to the use of multiple antenna. We further formulate the relationship between network density, antenna height, antenna array seize and carrier frequency showing how the coverage probability can be maintained with ultra-densification. From a system design perspective, we show that, if multiple antenna base stations are deployed at higher frequencies, monotonically increasing the coverage probability by means of ultra-densification is possible, and this without lowering the antenna height. Simulation results substantiate performance trends leveraging network densification and antenna deployment and configuration against path loss models and signal-to-noise plus interference thresholds.**

***Index Terms*— Network densification, MIMO, stochastic geometry, millimeter wave, antenna height, coverage probability, Fox's H-fading.**

I. Introduction

CHIEFLY urged by the unfolding mobile data deluge, a radical design make-over of cellular systems enabled by the so-called network densification and heterogeneity, primarily through the provisioning of small cells, has become an extremely active and promising research topic [2]–[10]. While small-cell densification has been recognized as a promising solution to boost capacity and enhance coverage with low cost and power-efficient infrastructure in 5G networks, it also paves the way for reliable and high capacity millimeter wave (mmWave) communication and directional beamforming [2]. Nevertheless, there has been noticeable divergence between the above outlook and conclusions of various studies on the fundamental limits of network densification, according to which the latter may eventually stop, at a certain point, delivering significant capacity gains [4]–[20].

In this respect, several valuable contributions leverage stochastic geometry (SG) to investigate ultra-dense networks performance under various path loss and propagation models [4], [5]. In the single-input single-output (SISO) context, conflicting findings based on various choices of path loss models have identified that the signal-to-noise plus interference (SINR) invariance property, which enables a potentially infinite aggregated data rate resulting from network densification based on the power-law model [4]–[11] vanishes once a more physically feasible path loss model is considered. In the latter case, [15]–[17] showed that the coverage probability attains a maximum point before starting to decay when the network becomes denser. Most recently, the authors of [17], [18] and [19] have investigated the limits of network densification when the path loss model includes the antenna height. Besides invalidating the SINR invariance property in this case, these works find that by lowering the antenna height the coverage drop due to ultra-densification can be totally offset, thereby improving the network capacity.

Motivated by the tractability of the considered system models, most of the previous works assumed the scenario of exponential-based distributions for the channel gains (e.g., integer fading parameter-based power series [6], [8], [14], and Laguerre polynomial series in [7]) and unbounded power law models, while the few noteworthy studies that incorporate general fading, shadowing and path loss models often lead to complex mathematical frameworks that fail to explicitly unveil the relationship between network density and system performance [5], [10], [11]. Moreover, although some works investigated the effect of path loss singularity [21]–[23] or boundedness [3], [9], the incorporation of the combined effect of path loss and generalized fading channel models is usually ignored. This has entailed divergent or even contrasting conclusions on the fundamental limits of network

Manuscript received July 11, 2020; revised November 16, 2020 and January 21, 2021; accepted February 17, 2021. Date of publication March 17, 2021; date of current version June 16, 2021. Work supported by the Discovery Grants and the CREATE PERSWADE (www.create-perswade.ca) programs of Natural Sciences and Engineering Research Council of Canada (NSERC) and a Discovery Accelerator Supplement (DAS) Award from NSERC. This work was also funded, in part, by the framework of the Competitiveness Enhancement Program of the Tomsk Polytechnic University, Russia. This article was presented in part at the IEEE Wireless Communications and Networking Conference (WCNC), Seoul, South Korea, April 6–9, 2020. The associate editor coordinating the review of this article and approving it for publication was J. Zhang. *(Corresponding author: Imène Trigui.)*

Imène Trigui is with the Département d'informatique, Université du Québec à Montréal, Montréal, QC H3T 1J4, Canada (e-mail: trigui.imen@courrier.uqam.ca).

Sofiène Affes is with the Institut National de la Recherche Scientifique, Centre Energie, Matériaux et Télécommunications, Montréal, QC H5A 1K6, Canada (e-mail: affes@emt.inrs.ca).

Marco Di Renzo is with the Laboratoire des Signaux et Systèmes, CentraleSupélec, CNRS, Université Paris-Saclay, 91192 Gif-sur-Yvette, France (e-mail: marco.di-renzo@universite-paris-saclay.fr).

Dushantha Nalin K. Jayakody is with the School of Computer Science and Robotics, Tomsk Polytechnic University (TPU), 634050 Tomsk, Russia, and also with the Centre for Telecommunications Research, School of Engineering, Sri Lanka Technological Campus (SLTC), Padukka 10500, Sri Lanka (e-mail: nalin@tpu.ru).

Color versions of one or more figures in this article are available at https://doi.org/10.1109/TCOMM.2021.3066583.

Digital Object Identifier 10.1109/TCOMM.2021.3066583

densification [3], [17], [18]. More importantly, additional work is necessary to investigate advanced communication and signal processing techniques, e.g., massive multiple-input-multiple-output (MIMO), coordinated multipoint (CoMP) and mmWave communications [24]–[26] that are expected to enhance the channel gain.

Motivated by the above background, we develop a comprehensive theoretical framework for analyzing the performance of dense networks over generalized fading channels. The main objective of this paper is, in particular, to introduce a non model-specific channel model that leads to a new unified approach to assess the performance of dense networks. To this end, we propose the Fox's H model as a unified fading distribution for a large number of widely used general multi-path and/or shadowing distributions. In particular, by leveraging fundamental results form the Fox's H transform theory and the Mellin-Barnes integrals along with SG, we investigate the performance limits of network densification under realistic path loss models and general channel power distributions, including propagation impediments and transmission gains due to the antenna pattern and beamforming, which are particularly relevant in multi-antenna settings. Several works [20]–[27] studied different performance metrics to characterize the performance of multi-antenna cellular networks, yet under the assumption of the standard power-law path loss model, since it leads to tractable analysis. In this paper, by leveraging a novel methodology of analysis that is compatible with a wide class of path loss models, including the antenna height, we are able to study the achievable performance of multi-antenna networks and understand how scaling the deployment density of the base stations (BSs) helps maintain the per user-coverage in dense networks. The main contributions of this paper are the following:

- A unified analytical framework characterizing the coverage performance and corresponding scaling laws of ad hoc and cellular networks under a general Fox's H distributed channel model with a smooth inclusion of both unbounded and bounded path loss models without the need of applying approximations or bounds.
- A low complexity extension to the multi-antenna scenario in both ad hoc and cellular networks enabling a more comprehensive investigation of the coverage performance. The asymptotic performance limits of multi-antenna networks are derived in closed-form showing that there is potential for improving the scaling laws of the coverage by increasing the number of BS antennas.
- Novel solutions to coverage decline due to densification by considering advanced transmission, such as MIMO and directional beamforming, and by considering the effect of high transmission frequencies (e.g., mmWave). We show that maintaining the maximum coverage is possible by deploying multiple antennas at the BS and by operating at higher frequency bands, and without lowering the BS height. The obtained scaling laws provide valuable system design guidelines for optimizing general networks deployment.

TABLE I
MAIN NOTATIONS AND MATHEMATICAL SYMBOLS/SHORTHAND

Symbol	Description
$\mathbb{R}^2$	Two-dimensional space.
$\mathbb{E}\{\cdot\}, \mathbb{P}(\cdot)$	Expectation and probability operators.
$\mathrm{H}_{p,q}^{u,v}[\cdot], \Gamma(\cdot)$	Fox's H and Gamma functions.
$\mathcal{L}_X, \mathcal{L}_X^{-1}$	Laplace transform of random variable X and its inverse.
α	Path loss exponent.
Φ_k, λ_k	Poisson Point Process (PPP) of tier-k BSs and density.
P_k	Transmit power of the k-th tier BSs.
g_{x_k}, g_{x_j}	Power gain of the channel from the k-th serving BS and x_k and from the j-th interfering BS at x_j to the typical user.
r_k, r_j	Distance from the typical user to the k-th serving BS to the j-th interfering BS.
$L(r)$	Path loss model.
β_k	SINR threshold of the k-th tier BSs.
σ^2	Thermal noise.

The rest of the paper is organized as follows. In Section II, we present the system model and the modeling assumptions. In Section III, we introduce our approach to obtain exact closed-form expressions and scaling laws for the coverage probability. Section IV is focused on multi-antenna BSs and single-antenna users, i.e., MISO networks. Applications of the obtained coverage expressions in different wireless communication scenarios are detailed in order to leverage the full potential of network densification. Numerical and simulation results are illustrated in Section V. Finally, Section VI concludes the paper.

II. SYSTEM MODEL

We consider the downlink transmission of a $\mathcal{T}$-tier heterogeneous wireless network. The BSs in Tier k, $k = 1, \ldots, \mathcal{T}$ are spatially distributed according to a homogenous Poisson point process (PPP) $\Phi_k \in \mathbb{R}^2$ with given spatial density $\lambda_k \geq 0$. We focus our attention on the performance analysis of a typical user equipment (UE) which is assumed, without loss of generality, to be located at the origin and is associated with BS $x_k \in \Phi_k$. Then, the SINR at the typical UE is formulated as

$$\mathrm{SINR}_k = \frac{L(r_k) g_{x_k}}{\sum_{i=1}^{\mathcal{T}} \sum_{x_i \in \Phi_i \setminus x_k} \widetilde{P}_i L(r_i) g_{x_i} + \sigma_k^2}, \qquad (1)$$

where the following notation is used:

- $L(r)$ is the path loss model, where $L(r) = r^{-\alpha}$ for an unbounded path loss and $L(r) = (1+r)^{-\alpha}$ for a bounded one.
- $\tilde{P}_i = \frac{P_i}{P_k}$ is the power of the i-th BS normalized by the power of the BS with index k serving the typical UE.
- σ_k^2 is the normalized noise power defined as $\sigma_k^2 = \frac{\sigma^2}{P_k}$.
- g_{x_k} is the channel power gain for the desired signal from the serving BS located at x_k. In this paper, a general type of distribution is assumed for g_{x_k} as follows.
  Assumption 1: The channel power gain g_{x_k} for the typical UE has a Fox's H distribution, i.e., $g_{x_k} \sim \mathrm{H}_{p,q}^{u,v}(x; \mathcal{P}_k)$, with the parameter sequence $\mathcal{P}_k = (\kappa_k, c_k, a_k, b_k, A_k, B_k)$ and probability density

function (pdf) [32]

$$f_{g_{x_k}}(x) = \kappa_k \mathrm{H}_{p,q}^{u,v}\left[c_k x \middle| \begin{matrix}(a_k, A_k)_p \\ (b_k, B_k)_q\end{matrix}\right], \quad x \geq 0. \quad (2)$$

where the Fox's H function is defined as [32, Eq. (1.2)]mathai

$$\mathrm{H}_{p,q}^{u,v}\left[z \middle| \begin{matrix}(a, A)_p \\ (b, B)_q\end{matrix}\right] = \frac{1}{2\pi i} \int_{\mathfrak{L}} \frac{\prod_{k=1}^{u}\Gamma(b_k+sB_k)\prod_{j=1}^{v}\Gamma(1-a_j-sA_j)z^{-s}}{\prod_{k=u+1}^{q}\Gamma(1-b_k-sB_k)\prod_{j=v+1}^{p}\Gamma(a_j+sA_j)} ds, \quad (3)$$

where $i = \sqrt{-1}$, $A_j > 0$ for all $j = 1, \ldots, p$, and $B_k > 0$, for all $k = 1, \ldots, q$ and $\mathfrak{L}$ is a suitable path of the integration that depends on the value of the parameters [32]. Examples of how classical and more recent fading models can fit into this unified fading model are provided in [34, Tables II-V]. In particular, the Fox's H function distribution captures composite effects of multipath fading and shadowing, subsuming a wide variety of important or generalized fading distributions adopted in wireless communications such as α-μ,[1] N-Nakagami-m, (generalized) $\mathcal{K}$-fading, Weibull/gamma, and the Fisher-Snedecor F-S $\mathcal{F}$ fading (see [33], [34], and [35] and references therein).

- α is the path loss exponent.
- g_{x_i} is the interferer's power gain from the interfering transmitter located at x_i. In the proposed framework, we assume that g_{x_i}, $i \in \{1, \ldots \mathcal{T}\}$ are non-negative random variables that are independent and identically distributed according to (2).

III. Unified Analytical Framework

In this section, we derive the complementary cumulative distribution function (ccdf) of the SINR, also called the coverage probability, in single-antenna networks. The obtained framework is utilized to analyze multi-antenna networks in general settings in the next section.

[1]The α-μ distributions can be attributed to exponential, one-sided Gaussian, Rayleigh, Nakagami-m, Weibull and Gamma fading distributions by assigning specific values for α and μ.

A. Coverage Analysis in Closest-BS-Association-Based Cellular Networks

Let the typical user be associated with the closest BS. This implies that the typical user is in coverage if the set $\mathcal{S} = \left\{\exists k \in \mathcal{T} : k = \arg\max_{j\in\mathcal{T}, x\in\Phi_j} \widetilde{P}_j L(r_j); \mathrm{SINR}_k \geq \beta_k\right\}$ is not empty.

Proposition 1: When the locations of the BSs are modeled as a Poisson point process (PPP) [13] and the nearest-BS association is adopted, the SINR coverage probability at the typical UE for an unbounded path loss model and the SINR thresholds β_k, $k \in \{1, \ldots, \mathcal{T}\}$, is given by

$$\mathcal{C}^{\mathcal{U}} = \pi\delta \sum_{k=1}^{\mathcal{T}} \frac{\lambda_k}{\sigma_k^{2\delta}} \int_0^{\infty} \frac{1}{\xi^{2+\delta}} \mathrm{H}_{q,p+1}^{v,u}\left(\xi, \mathcal{P}_{\mathcal{U}}^{k}\right) \mathrm{H}_{1,1}^{1,1}\left(\frac{\pi}{(\xi\sigma_k^2)^{\delta}} \sum_{j=1}^{\mathcal{T}} \lambda_j \widetilde{P}_j^{\delta}\left(1+\delta\xi \mathrm{H}_{q+2,p+3}^{v+1,u+2}\left(\xi, \mathcal{P}_{\mathcal{U}}^{\mathcal{I}_j}\right)\right), \mathcal{P}_{\delta}\right) d\xi, \quad (4)$$

where $\delta = \frac{2}{\alpha}$, $\mathcal{P}_{\delta} = (1, 1, 1-\delta, 0, \delta, 1)$, with

$$\mathcal{P}_{\mathcal{U}}^{k} = \left(\kappa_k\beta_k, \frac{1}{c_k\beta_k}, 1-b_k, (1-a_k, 1), B_k, (A_k, 1)\right), \quad (5)$$

and

$$\mathcal{P}_{\mathcal{U}}^{\mathcal{I}_j} = \Bigg(\frac{\kappa_j}{c_j^2}, \frac{1}{c_j}, (1-b_j-2B_j, 0, \delta), (0, 1-a_j-2A_j, -1, \delta-1), \times (B_j, 1, 1), (1, A_j, 1, 1)\Bigg). \quad (6)$$

Proof: See Appendix A.

The main assumptions in Proposition 1 are the Fox's H distributed signal and interference channel power gains and the standard power-law unbounded path loss model. The unbounded power-law path loss is known to be inaccurate for short distances, due to the singularity at the origin, which affects the scaling laws of the coverage probability [21]. Next, a more physically feasible path loss model is considered.

Proposition 2: When a bounded path loss model is adopted, the coverage probability of cellular networks based on the nearest-BS association strategy is given in (7)-(9), as shown at the bottom of the page, that are shown at the top of the next page.

Proof: See Appendix B.

Remark 1: For arbitrary distributions for the channel gain, the coverage expressions in (4) and (7) are independent of the

$$\mathcal{C}^{\mathcal{B}} = \sum_{k=1}^{\mathcal{T}} \lambda_k \int_0^{\infty} e^{-\sum_{j\in\mathcal{T}} \pi\lambda_j \widetilde{P}_j^{\delta} \delta\xi(\Psi_1-\Psi_2)} \frac{\mathrm{H}_{q,p+1}^{v,u}\left(\xi, \mathcal{P}_{\mathcal{B}}^{k}\right)}{\xi^2 \sum_{j=1}^{\mathcal{T}} \pi\lambda_j \widetilde{P}_j^{\delta} \delta\xi(\Psi_1+\Psi_2)} \mathrm{H}_{1,1}^{1,1}\left(\frac{\sum_{j=1}^{\mathcal{T}} \lambda_j \widetilde{P}_j^{\delta}\left(1+\delta\xi\Psi_1\right)}{\sum_{j=1}^{\mathcal{T}} \lambda_j \widetilde{P}_j^{\delta} \delta\xi(2\Psi_1+\Psi_2)}, \widetilde{\mathcal{P}}_{\delta}\right) d\xi, \quad (7)$$

where $\widetilde{\mathcal{P}}_{\delta} = (1, 1, -1, 0, 2, 1)$, $\mathcal{P}_{\mathcal{B}}^{k} = \mathcal{P}_{\mathcal{U}}^{k}$ and $\Psi_x = \mathrm{H}_{q+2,p+3}^{v+1,u+2}\left(\xi, \mathcal{P}_{\mathcal{B}}^{x,\mathcal{I}}\right), x \in \{1, 2\}$ with

$$\mathcal{P}_{\mathcal{B}}^{1,j,\mathcal{I}} = \left(\frac{\kappa_j}{c_j^2}, \frac{1}{c_j}, (1-b_j-2B_j, 0, \delta), (0, 1-a_j-2A_j, -1, \delta-1), (B_j, 1, 1), (1, A_j, 1, 1)\right) \quad (8)$$

and

$$\mathcal{P}_{\mathcal{B}}^{2,j,\mathcal{I}} = \left(\frac{\kappa_j}{c_j^2}, \frac{1}{c_j}, \left(1-b_j-2B_j, 0, \frac{\delta}{2}\right), \left(0, 1-a_j-2A_j, -1, \frac{\delta}{2}-1\right), (B_j, 1, 1), (1, A_j, 1, 1)\right) \quad (9)$$

TABLE II

COVERAGE PROBABILITY OF SOME WELL-KNOWN FADING CHANNEL MODELS BASED ON THE CLOSEST-BS STRATEGY

Instantaneous Fading Distribution	**Coverage Probability $\mathcal{C}^{\mathcal{U}}$**
Gamma Fading $f_g(z) = \frac{m}{\Gamma(m)} \mathrm{H}_{0,1}^{1,0}\left[mz \middle\vert \begin{matrix} - \\ (m-1,1) \end{matrix} \right]$	$\mathcal{C}^{\mathcal{U}} = \pi\delta \sum_{k=1}^{\mathcal{T}} \frac{\lambda_k m_k \beta_K}{\Gamma(m_k)} \left(\frac{P_k}{\sigma_k^2}\right)^{\delta} \int_0^{\infty} \frac{\mathrm{H}_{1,1}^{0,1}\left[\frac{\xi}{m_k\beta_k} \middle\vert \begin{matrix} (2-m_k,1) \\ (1,1) \end{matrix} \right]}{\xi^{2+\delta}}$ $\mathrm{H}_{1,1}^{1,1}\left(\frac{\left(\frac{P_k}{\sigma_k^2}\right)^{\delta}}{\xi^{\delta}} \sum_{j=1}^{\mathcal{T}} \pi\lambda_j \widetilde{P}_j^{\delta} \left(1 + \frac{\delta\xi}{m_j\Gamma(m_j)} \mathrm{H}_{3,3}^{1,3}\left[\frac{\xi}{m_j} \middle\vert \begin{matrix} (-m_j,1),(0,1),(\delta,1) \\ (0,1),(-1,1),(\delta-1,1) \end{matrix} \right] \right), \mathcal{P}_{\delta} \right) d\xi$
Generalized Gamma $f_g(z) = \frac{\mu}{\Gamma(m)} \mathrm{H}_{0,1}^{1,0}\left[\mu z \middle\vert \begin{matrix} - \\ (m-\frac{1}{\eta},\frac{1}{\eta}) \end{matrix} \right]$ where $\mu = \frac{\Gamma(m+\frac{1}{\eta})}{\Gamma(m)}$.	$\mathcal{C}^{\mathcal{U}} = \pi\delta \sum_{k=1}^{\mathcal{T}} \frac{\lambda_k \mu_k \beta_K}{\Gamma(m_k)} \left(\frac{P_k}{\sigma_k^2}\right)^{\delta} \int_0^{\infty} \frac{\mathrm{H}_{1,1}^{0,1}\left[\frac{\xi}{\mu_k\beta_k} \middle\vert \begin{matrix} (1+\frac{1}{\eta_k}-m_k,\frac{1}{\eta_k}) \\ (1,1) \end{matrix} \right]}{\xi^{2+\delta}}$ $\mathrm{H}_{1,1}^{1,1}\left(\frac{\left(\frac{P_k}{\sigma_k^2}\right)^{\delta}}{\xi^{\delta}} \sum_{j=1}^{\mathcal{T}} \pi\lambda_j \widetilde{P}_j^{\delta} \left(1 + \frac{\delta\xi}{\mu_j\Gamma(m_j)} \mathrm{H}_{3,3}^{1,3}\left[\frac{\xi}{\mu_j} \middle\vert \begin{matrix} (1-\frac{1}{\eta_j}-m_j,1),(0,1),(\delta,1) \\ (0,1),(-1,1),(\delta-1,1) \end{matrix} \right] \right), \mathcal{P}_{\delta} \right) d\xi$
Power of Nakagami-n (Rice) $f_g(z) = \sum_{k=0}^{\infty} \frac{\Psi_k m_k}{\Gamma(m_k)\Omega_k} \mathrm{H}_{0,1}^{1,0}\left[\frac{m_k}{\Omega_k} z \middle\vert \begin{matrix} - \\ (m_k-1,1) \end{matrix} \right]$ with $m_k = k+1$ and $\Omega_k = \frac{k+1}{1+K_R}$, where K_R is the Rician factor.	$\mathcal{C}^{\mathcal{U}} = \pi\delta \sum_{k=1}^{\mathcal{T}} \lim_{K_k \longrightarrow \infty} \sum_{t=0}^{K_k} \frac{\Psi_t m_t}{\Gamma(m_t)\Omega_t\lambda_k\beta_k} \left(\frac{P_k}{\sigma_k^2}\right)^{\delta} \int_0^{\infty} \frac{\mathrm{H}_{1,1}^{0,1}\left[\frac{\xi\Omega_t}{m_t\beta_k} \middle\vert \begin{matrix} (2-m_t,1) \\ (1,1) \end{matrix} \right]}{\xi^{2+\delta}}$ $\mathrm{H}_{1,1}^{1,1}\left(\frac{\left(\frac{P_k}{\sigma_k^2}\right)^{\delta}}{\xi^{\delta}} \sum_{j=1}^{\mathcal{T}} \pi\lambda_j \widetilde{P}_j^{\delta} \left(1 + \sum_{t=0}^{\infty} \frac{\Psi_t\Omega_t\delta\xi}{\Gamma(m_t)m_t} H_{3,3}^{1,3}\left[\frac{\xi\Omega_t}{m_t} \middle\vert \begin{matrix} (-m_t,1),(0,1),(\delta,1) \\ (0,1),(-1,1),(\delta-1,1) \end{matrix} \right] \right), \mathcal{P}_{\delta} \right) d\xi$, where $\Psi_k = K_R^k e^{-K_R}/\Gamma(k+1)$.
Lognormal Fading $f_g(z) = \sum_{n=0}^{N} \frac{w_n}{\omega_n} \mathrm{H}_{0,0}^{0,0}\left[\frac{z}{\omega_n} \middle\vert \begin{matrix} - \\ - \end{matrix} \right]$ where $\omega_n = 10^{\sqrt{2}\sigma u_n + \mu}$, while u_n and w_n represent the weight factors and the zeros of the N-order Hermite polynomial [6, Table 25.10].	$\mathcal{C}^{\mathcal{U}} = \pi\delta \sum_{k=1}^{\mathcal{T}} \sum_{t=0}^{N_k} \frac{w_t}{\omega_t\lambda_k\beta_k} \left(\frac{P_k}{\sigma_k^2}\right)^{\delta} \int_0^{\infty} \frac{\mathrm{H}_{0,1}^{0,0}\left[\frac{\xi\omega_t}{\beta_k} \middle\vert \begin{matrix} - \\ (1,1) \end{matrix} \right]}{\xi^{2+\delta}}$ $\mathrm{H}_{1,1}^{1,1}\left(\frac{\left(\frac{P_k}{\sigma_k^2}\right)^{\delta}}{\xi^{\delta}} \sum_{j=1}^{\mathcal{T}} \pi\lambda_j \widetilde{P}_j^{\delta} \left(1 + \sum_{t=0}^{N_j} \frac{w_t\delta\xi}{\omega_t^2} \mathrm{H}_{2,3}^{1,2}\left[\xi\omega_t \middle\vert \begin{matrix} (0,1),(\delta,1) \\ (0,1),(-1,1),(\delta-1,1) \end{matrix} \right] \right), \mathcal{P}_{\delta} \right) d\xi$
Fisher-Snedecor Fading $f_g(z) = \frac{m}{m_s\Gamma(m_s)\Gamma(m)} \mathrm{H}_{1,1}^{1,1}\left[\frac{mz}{m_s} \middle\vert \begin{matrix} (-m_s,1) \\ (m-1,1) \end{matrix} \right]$	$\mathcal{C}^{\mathcal{U}} = \pi\delta \sum_{k=1}^{\mathcal{T}} \frac{\lambda_k m_k \beta_K}{m_{s_k}\Gamma(m_k)\Gamma(m_{s_k})} \left(\frac{P_k}{\sigma_k^2}\right)^{\delta} \int_0^{\infty} \frac{\mathrm{H}_{1,2}^{1,1}\left[\frac{\xi m_{s_k}}{m_k\beta_k} \middle\vert \begin{matrix} (2-m_k,1) \\ (1+m_{s_k},1),(1,1) \end{matrix} \right]}{\xi^{2+\delta}}$ $\mathrm{H}_{1,1}^{1,1}\left(\frac{\left(\frac{P_k}{\sigma_k^2}\right)^{\delta}}{\xi^{\delta}} \sum_{j=1}^{\mathcal{T}} \pi\lambda_j \widetilde{P}_j^{\delta} \left(1 + \frac{\delta\xi}{m_j\Gamma(m_j)} \mathrm{H}_{3,3}^{1,3}\left[\frac{\xi}{m_j} \middle\vert \begin{matrix} (-m_j,1),(0,1),(\delta,1) \\ (0,1),(-1,1),(\delta-1,1) \end{matrix} \right] \right), \mathcal{P}_{\delta} \right) d\xi$

n-th derivative of the Laplace transform of the aggregate interference, $n \in [0,\infty)$, while accurately reflecting the behavior of multi-tiers networks in all operating regimes without the need of applying approximations or upper bounds. Compared with the coverage approximations in [7], [8], and [14] and expressions in [5], [6], the proposed approach yields a more compact analytical result for the coverage probability, where only an integration of Fox's H functions is needed thanks to the novel handling of fading distributions. Table II lists some commonly-used channel fading distributions and the corresponding expression for $\mathcal{C}$.

It is worth noting that the proposed framework can be extended to other network models, for example, where the transmitters are spatially distributed according to other point processes [36], [37], notably including non-Poisson models [23], or under multi-slope path loss models [16], [22]. Hence, the results of this paper allow for an exact and tractable approximation of the coverage probability of any stationary and ergodic point process [23], [36]. In the next section, we show the usefulness of the proposed approach for obtaining insightful design guidelines for multi-antenna and mmWave networks.

B. Coverage Analysis in Strongest-BS-Association-Based Cellular Networks

The strongest-BS association rule, according to which the serving BS is the one that provides the maximum

signal-to-interference (SIR),[2] can be particularly advantageous for application to scenarios in which the closest-BS association strategy may provide poor performance due to severe blockages. Also, the strongest-BS association criterion may yield performance bounds for other, more practical, cell association strategies. Under the strongest-BS association, the typical user is in coverage if the set $\mathcal{S} = \left\{ \exists k \in \mathcal{T}; \max_{x_k \in \Phi_k} \text{SIR}_k \geq \beta_k \right\}$ is not empty [14].

Proposition 3: When the strongest-BS association is adopted, the SIR coverage probability of the typical UE with unbounded path loss model, given the SIR thresholds β_k, $k \in \{1, \ldots, \mathcal{T}\}$, is given by

$$\mathcal{C} = 2\pi \sum_{k=1}^{\mathcal{T}} \frac{\kappa_k \lambda_k}{c_k} \int_0^{\infty} r_k \Upsilon(r_k) d_{r_k} = \frac{\pi}{C(\delta)} \sum_{k=1}^{\mathcal{T}} \frac{\lambda_k \beta_k^{-\delta} \Lambda_k}{\sum_{j \in \mathcal{T}} \lambda_j \widetilde{P}_j^{\delta} \Lambda_j}, \tag{10}$$

with

$$\Upsilon(r_k) = \mathrm{H}_{p+1,q+1}^{u+1,v} \left[\sum_{j=1}^{\mathcal{T}} \frac{\pi r_k^2 \lambda_j \Gamma(1-\delta) \Lambda_j}{\widetilde{P}_j^{-\delta} (c_k \beta_k)^{-\delta}} \middle| \begin{matrix} (a_k + A_k, \delta A_k), (1, \delta) \\ (0,1), (b + B_k, \delta B_k) \end{matrix} \right], \tag{11}$$

where $C(\delta) = \pi^2 \delta \csc(\pi\delta)$ and

$$\Lambda_j = \frac{\kappa_j}{c_j^{\delta+1}} \frac{\prod_{t=1}^{u} \Gamma\left(b_{j_t} + (1+\delta) B_{j_t}\right)}{\prod_{t=u+1}^{p} \Gamma\left(1 - b_{j_t} - (1+\delta) B_{j_t}\right)} \times \frac{\prod_{k=1}^{v} \Gamma\left(1 - a_{j_k} - (1+\delta) A_{j_k}\right)}{\prod_{k=v+1}^{p} \Gamma\left(a_{j_k} + (1+\delta) A_{j_k}\right)}. \tag{12}$$

Proof: The proof follows from Appendix C along with the fact that

$$\mathbb{E}_{r_k}\left[\Upsilon(r_k)\right] = 2\pi\lambda_k \int_0^{\infty} r_k \mathrm{H}_{p+1,q+1}^{u+1,v} \left[\sum_{j=1}^{\mathcal{T}} \frac{\pi r_k^2 \lambda_j \Gamma(1-\delta) \Lambda_j}{\widetilde{P}_j^{-\delta} (c_k \beta_k)^{-\delta}} \middle| \begin{matrix} (a_k + A_k, \delta A_k), (1, \delta) \\ (0,1), (b + B_k, \delta B_k) \end{matrix} \right] d_{r_k}. \tag{13}$$

Then, applying the transformation $\mathrm{H}_{p,q}^{m,n}\left[x \middle| \begin{matrix} (a_i, kA_j)_p \\ (b_i, kB_j)_q \end{matrix}\right] = \frac{1}{k} \mathrm{H}_{p,q}^{m,n}\left[x^{\frac{1}{k}} \middle| \begin{matrix} (a_i, A_j)_p \\ (b_i, B_j)_q \end{matrix}\right]$, $k > 0$ and the Mellin transform in [32], we obatin

$$\mathbb{E}_{r_k}\left[\Upsilon(r_k)\right] = \frac{\Gamma(1-\delta)^{-1}}{\Gamma(1+\delta)} \frac{c_k \beta_k^{-\delta} \frac{\Lambda_k}{\kappa_k}}{\sum_{j \in \mathcal{T}} \lambda_j \widetilde{P}_j^{\delta} \Lambda_j}. \tag{14}$$

Finally, plugging (14) into (10) yields the desired result after some manipulations.

Remark 2: As shown in (10), the main task in deriving the coverage probability in cellular networks under the strongest-BS cell association criterion is to calculate Λ. In Table III, we show the coverage probability for the strongest-BS association criterion when various special cases of the Fox's H function distribution are considered. Notably, (10) is instrumental in evaluating the impact of the number of tiers or their relative densities, transmit powers, and target SIR over generalized fading scenarios. This result complements existing valuable coverage studies of cellular networks over generalized fading [14, Proposition 1], [9, Corollary 1].

Remark 3: Our proposed method in Proposition 3 can be exploited to smoothly include the bounded path loss model into the coverage analysis. From a computational perspective, we note that closed-form expressions in this case may not be affordable due to a double integration. Due to space limitations, the details are omitted. In particular, we only report the unbounded case since it allows useful coverage simplifications.

C. Coverage Analysis in Ad Hoc Networks

Ad hoc networks with short-range transmission are, from an architecture perspective, similar to device-to-device (D2D) communication networks where Internet of Things (IoT) devices communicate directly over the regular cellular spectrum but without using the BSs. We use the dipole PPP model [40] where the typical receiver has its associated transmitter in the k-th tier at a fixed distance r_k, assumed to be independent of the set of interfering transmitters and their densities.[3]

Proposition 4: The coverage probability of ad hoc networks over the Fox's H fading channel is given by

$$\mathcal{C} = \sum_{k=1}^{\mathcal{T}} \frac{\kappa_k}{c_k} \Upsilon(r_k), \tag{15}$$

where $\Upsilon(r_k)$ is given in (11).

Proof: It follows from Proposition 3 when r_k is fixed.

We note that the coverage probability in ad hoc networks involves a finite summation of Fox's H functions which can be efficiently evaluated [11]. Overall, the obtained analytical expressions are easier to compute than existing results [4]–[6], [17]–[20] that contain multiple nested integrals.

D. The Impact of Network Densification

In this section, we exploit the derived analytical framework to analyze the coverage scaling laws for single-antenna multi-tiers cellular and ad hoc networks. Assuming $\lambda_k = \lambda \to \infty$, $k = 1, \ldots, \mathcal{T}$, the coverage scaling laws are given in the following text.

1) Coverage Scaling Law in Cellular Networks: The coverage probability of single antenna-cellular networks with an unbounded path loss model is invariant with the BS density λ. Specifically, we have

$$\mathcal{C}^{\mathcal{U},\infty} = \sum_{k=1}^{\mathcal{T}} \int_0^{\infty} \frac{\mathrm{H}_{q,p+1}^{v,u}\left(\xi, \mathcal{P}_{\mathcal{U}}^k\right) d\xi}{\xi^2 \sum_{j=1}^{\mathcal{T}} \widetilde{P}_j^{\delta} \left(1 + \delta\xi \mathrm{H}_{q+2,p+3}^{v+1,u+2}\left(\xi, \mathcal{P}_{\mathcal{U}}^{\mathcal{T}}\right)\right)}, \tag{16}$$

which is obtained by letting $\lambda \to \infty$ in Proposition 1 and resorting to the asymptotic expansion of the Fox's H function $\mathrm{H}_{1,1}^{1,1}(x; \mathcal{P}_{\delta}) \underset{x \to \infty}{\approx} \frac{1}{\delta} x^{-1}$ along with applying [38, Eq.(1.5.9)].

[2] [9] showed that self-interference dominates noise in typical heterogeneous networks under the strongest-BS association. Therefore, we ignore noise in the rest of this section.

[3] The dipole PPP model is perhaps simplistic, but we leave the investigation of random wireless ad hoc networks with mobile nodes and with clustered and non-homogeneous PPPs [37] to future work.

TABLE III

COVERAGE PROBABILITY OF SOME WELL-KNOWN FADING CHANNEL MODELS BASED ON THE STRONGEST-BS ASSOCIATION

Instantaneous Fading Distribution	Coverage Probability $\mathcal{C}^{\mathcal{U}}$
Gamma Fading	$\mathcal{C}^{\mathcal{U}} = \frac{\pi}{C(\delta)} \sum_{k=1}^{\mathcal{T}} \frac{\lambda_k \beta_k^{-\delta} \frac{\Gamma(m_k+\delta)}{\Gamma(m_k) m_k^{\delta}}}{\sum_{j=1}^{\mathcal{T}} \lambda_j \widetilde{P}_j^{\delta} \frac{\Gamma(m_j+\delta)}{\Gamma(m_j) m_j^{\delta}}}$.
Generalized Gamma	$\mathcal{C}^{\mathcal{U}} = \frac{\pi}{C(\delta)} \sum_{k=1}^{\mathcal{T}} \frac{\lambda_k \beta_k^{-\delta} \frac{\Gamma(\mu_k)^{\delta-1}}{\Gamma\left(\mu_k+\frac{1}{\alpha_k}\right)^{\delta}} \Gamma\left(\mu_k+\frac{\delta}{\alpha_k}\right)}{\sum_{j=1}^{\mathcal{T}} \lambda_j \widetilde{P}_j^{\delta} \frac{\Gamma(\mu_j)^{\delta-1}}{\Gamma\left(\mu_j+\frac{1}{\alpha_j}\right)^{\delta}} \Gamma\left(\mu_j+\frac{\delta}{\alpha_j}\right)}$.
Power of Nakagami-n (Rice)	$\mathcal{C}^{\mathcal{U}} = \frac{\pi}{C(\delta)} \sum_{k=1}^{\mathcal{T}} \frac{\lambda_k \beta_k^{-\delta} e^{-K_{R_k}} \sum_{t=0}^{\infty} \frac{K_{R_k}^t \Gamma(m_t+\delta)}{\Gamma(t+1)\Gamma(m_t)} \left(\frac{\Omega_t}{m_t}\right)^{\delta}}{\sum_{j=1}^{\mathcal{T}} \lambda_j e^{-K_{R_j}} \widetilde{P}_j^{\delta} \sum_{t=0}^{\infty} \frac{K_{R_j}^t \Gamma(m_t+\delta)}{\Gamma(t+1)\Gamma(m_t)} \left(\frac{\Omega_t}{m_t}\right)^{\delta}}$.
Lognormal Fading	$\mathcal{C}^{\mathcal{U}} = \frac{\pi}{C(\delta)} \sum_{k=1}^{\mathcal{T}} \frac{\lambda_k \beta_k^{-\delta} \sum_{n=0}^{N_k} w_n 10^{\delta(\sqrt{2}\sigma_k u_n + \mu_k)}}{\sum_{j=1}^{\mathcal{T}} \lambda_j \widetilde{P}_j^{\delta} \sum_{n=0}^{N_j} w_n 10^{\delta(\sqrt{2}\sigma_j u_n + \mu_j)}}$.
Fisher-Snedecor Fading	$\mathcal{C}^{\mathcal{U}} = \frac{\pi}{C(\delta)} \sum_{k=1}^{\mathcal{T}} \frac{\lambda_k \beta_k^{-\delta} \frac{m_{s_k}^{\delta} \Gamma(m_k+\delta)\Gamma(m_{s_k}-\delta)}{\Gamma(m_{s_k})\Gamma(m_k) m_k^{\delta}}}{\sum_{j=1}^{\mathcal{T}} \lambda_j \widetilde{P}_j^{\delta} \frac{m_{s_j}^{\delta} \Gamma(m_j+\delta)\Gamma(m_{s_j}-\delta)}{\Gamma(m_{s_j})\Gamma(m_j) m_j^{\delta}}}$.

We note that (16) generalizes the SINR invariance property that has been revealed in some specific settings, e.g., [3], [4], [5], and [9].

Contrary to what the standard unbounded path loss model predicts, the coverage probability under the bounded path loss model scales with $e^{-\lambda}$ and approaches zero with increasing λ for general values of δ. This is readily shown in the following asymptotic coverage expression obtained by letting $\lambda \to \infty$ in Proposition 2, as[4]

$$\mathcal{C}^{\mathcal{B},\infty} = \sum_{k=1}^{\mathcal{T}} \int_0^{\infty} e^{-\lambda \sum_{j=1}^{\mathcal{T}} \pi \widetilde{P}_j^{\delta} \delta\xi(\Psi_1 - \Psi_2)} \times \frac{\mathrm{H}_{q,p+1}^{v,u}\left(\xi, \mathcal{P}_{\mathcal{B}}^k\right) \mathrm{H}_{1,1}^{1,1}\left(\frac{\sum_{j=1}^{\mathcal{T}} \widetilde{P}_j^{\delta}(1+\delta\xi\Psi_1)}{\sum_{j\in\mathcal{T}} \widetilde{P}_j^{\delta} \delta\xi(2\Psi_1+\Psi_2)}, \mathcal{P}_{\delta}\right)}{\xi^2 \sum_{j=1}^{\mathcal{T}} \pi \widetilde{P}_j^{\delta} \delta\xi(\Psi_1+\Psi_2)} d\xi. \quad (17)$$

Due to the complexity of the bounded model, the impact of λ was only understood through approximations in [14] and [15] and for fading scenarios with integer parameters. Thanks to our proposed unified approach, the impact of ultra densification can be scrutinized in the most comprehensive setting of multi-tier networks under the Fox's H fading channel.

2) Coverage Scaling Law in Ad Hoc Networks: In ad hoc networks, to the best of our knowledge, there exists no works that quantified the effect of densification over generalized fading channels. By exploiting the proposed analytical framework, the coverage scaling law in ad hoc networks is revealed in this paper. First, it is pertinent to remark that $g_k \sim \text{H-}\{(q,0,p,q),\mathcal{P}\}$ can be assumed in the majority of fading distributions as shown in Table II. In this case, applying the asymptotic expansion of the Fox's H function [38, Eq. (1.7.14)] $\mathrm{H}_{p,q}^{q,0}(x) \sim x^{\frac{\nu+\frac{1}{2}}{\Delta}} \exp\left[-\Delta\left(\frac{x}{\rho}\right)^{1/\Delta}\right]$ to (15), we obtain

$$\mathcal{C} \underset{\lambda\to\infty}{\approx} \sum_{k=1}^{\mathcal{T}} \frac{\kappa_k}{c_k} (\lambda\mathcal{A})^{\frac{\nu_k+\frac{1}{2}}{\Delta_k}} \exp\left[-\Delta_k\left(\lambda\frac{\mathcal{A}}{\rho_k}\right)^{1/\Delta_k}\right], \quad (18)$$

where $\mathcal{A} = \sum_{j=1}^{\mathcal{T}} \frac{\pi r_k^2 \Gamma(1-\delta)\Lambda_j}{\widetilde{P}_j^{-\delta}(c_k\beta_k)^{-\delta}}$, $\Delta_k = 1 + \delta\left(\sum_{j=1}^{q} B_{j_k} - \sum_{j=1}^{p} A_{j_k} - 1\right)$, $\rho_k = \delta^{\delta} \prod_{j=1}^{p} (\delta A_{j_k})^{-\delta A_{j_k}} \prod_{j=1}^{q} (\delta B_{j_k})^{-\delta B_{j_k}}$, and $\nu_k = \sum_{j=1}^{q} b_{j_k} - \sum_{j=1}^{p} a_{j_k} + \sum_{j=1}^{q} B_{j_k} - \sum_{j=1}^{p} A_{j_k} + \frac{p-q}{2} - 1$ are constants defined in [38, Eq. (1.1.8)], [38, Eq. (1.1.9)], and [38, Eq. (1.1.10)], respectively.

In the special case of Gamma fading, i.e., $g_{x_k} \sim \texttt{Gamma}(m_k,1) \sim \text{H-}\{(1,0,0,1),\mathcal{P}\}$, it can be shown that $\Delta_k = 1$, $\rho_k = 1$, and $\nu_k = m_k - \frac{3}{2}$, which results in

$$\mathcal{C} \underset{\lambda\to\infty}{\approx} \sum_{k=1}^{\mathcal{T}} \frac{(\lambda\mathcal{A})^{m_k-1}}{\Gamma(m_k)} \exp(-\lambda\mathcal{A}). \quad (19)$$

It turns out that the coverage probability of ad hoc networks in arbitrary Nakagami-m fading (i.e., $g_{x_k} \sim \texttt{Gamma}(m_k,1)$, $k = 1,\ldots,\mathcal{T}$) is formulated as the product of an exponential

[4]Using the Mellin-Barnes integral representations of Ψ_1 and Ψ_2 [32], we can easily show that $\Psi_1 - \Psi_2 > 0$.

function and a polynomial function of order $\mathcal{T}(\max_{k=1,\ldots,\mathcal{M}} m_k - 1)$ of the transmitter density λ. When $\mathcal{T} = 1$, i.e., in single-tier networks, the coverage probability is a product of an exponential function and a power function of order $m-1$. In the special case when $\mathcal{T} = m = 1$, i.e., in single-tier ad hoc networks over a Rayleigh fading channel, the coverage probability reduces to an exponential function.

IV. Multi-Antenna Vs. Single-Antenna Networks

A. Coverage Analysis

In multi-antenna networks, the analysis of the coverage probability is more difficult due to the more complicated signal and interference distributions. However, we emphasize that, for several MIMO techniques, the associated post-processing signal power gain can include Gamma-type fading [20], [25], [27], [28] with $g_x \sim \texttt{Gamma}(M, \theta)$ where M is typically related to the number of antennas (e.g. $M = N_t, \theta = 1$ for maximum-ratio-transmission (MRT) and $M = N_t, \theta = 1/N_t$ for millimeter wave analog beamforming, where N_t is the number of antennas at the transmitter) [27, Table II]. Hence, assuming that the signal power is gamma distributed in multi-antenna networks and recognizing that $f_{g_x}(x) = \frac{\theta^{-1}}{\Gamma(M)} \mathrm{H}_{0,1}^{1,0}\left[\frac{x}{\theta}\middle| \begin{matrix} - \\ (M-1,1)\end{matrix}\right]$, then the Fox's H-based modeling of the coverage presented in Section III can be generalized to the analysis of muti-anetnna networks.

1) Multi-Antenna Cellular Networks: We consider multiple-input-single-output (MISO) networks using MRT where the BSs of the k-th tier are equipped with N_{t_k} antennas. We assume that the channel power gain g_{x_k} of the desired signal is gamma distributed such that $g_{x_k} \sim \texttt{Gamma}(N_{t_k}, 1)$ [27]. As far as the interference distribution is concerned, we assume that g_{x_i} are identically distributed according to an arbitrary Fox's H distribution. Hence, Proposition 1 can be generalized to obtain the coverage probability in multi-antenna cellular networks with arbitrary interference, as

$$\mathcal{C} = \pi\delta \sum_{k=1}^{\mathcal{T}} \frac{\left(\frac{P_k}{\sigma_k^2}\right)^{\delta} \lambda_k \beta_K}{\Gamma(N_{t_k})} \int_0^{\infty} \frac{\eta(\xi)}{\xi^{2+\delta}} \mathrm{H}_{1,1}^{0,1}\left[\frac{\xi}{\beta_k}\middle| \begin{matrix} (2-N_{t_k},1] \\ (1,1)\end{matrix}\right] d\xi, \tag{20}$$

where

$$\eta(\xi) = \mathrm{H}_{1,1}^{1,1}\left(\sum_{j=1}^{\mathcal{T}} \frac{\pi\lambda_j \widetilde{P}_j^{\delta}}{\left(\frac{P_k}{\xi\sigma_k^2}\right)^{-\delta}} \left(1 + \delta\xi \mathrm{H}_{q+2,p+3}^{v+1,u+2}\left(\xi, \mathcal{P}_{\mathcal{U}}^{\mathcal{I}_j}\right)\right), \mathcal{P}_{\delta}\right). \tag{21}$$

Compared with existing approaches in [20]–[26], which requires the calculation of $N_{t_k} - 1$ derivatives of $\eta(\xi)$ when g_{x_k} is gamma distributed as $\texttt{Gamma}(N_{t_k}, 1)$, the framework in (20) and (21) adds no computational complexity and thus preserves the tractability of single-antenna settings. We note that assuming a Gamma distribution for the interferers' power gain, i.e. $g_{x_j} \sim \texttt{Gamma}(\chi_j, \phi_j)$, $j \in \{1, \ldots, \mathcal{T}\}$, is commonly encountered in multi-antenna networks [27], [30], [31]. In this case, we only need to modify the parameters of $\eta(\xi)$ by replacing in (20) the following equation

$$\mathcal{P}_{\mathcal{U}}^{\mathcal{I},j} = \Bigg(\frac{\phi_j}{\Gamma(\chi_j)}, \phi_j, (-\chi_j, 0, \delta), (0, 1, , \delta - 1), (1,1,1), (1,1,1,1)\Bigg). \tag{22}$$

2) Multi-Antenna Ad Hoc Networks: The coverage probability of ad hoc networks for different multi-antenna transmission strategies for which $g_{x_k} \sim \texttt{Gamma}(M_k, \theta_k)$, $k = 1, \ldots, \mathcal{T}$ is directly obtained from (15) as

$$\mathcal{C} = \sum_{k=1}^{\mathcal{T}} \frac{1}{\Gamma(M_k)} \times \mathrm{H}_{1,2}^{2,0}\left[\sum_{j=1}^{\mathcal{T}} \frac{\pi r_k^2 \lambda_j \Gamma(1-\delta)\Lambda_j \beta_k^{\delta}}{\widetilde{P}_j^{-\delta} (\theta_k)^{-\delta}} \middle| \begin{matrix} (1,\delta) \\ (0,1), (M_k, \delta)\end{matrix}\right], \tag{23}$$

where Λ_j accounts for Fox's H identically distributed interferences and is given in (12). The coverage probability scaling law of multi-antenna ad hoc networks using MRT with N_{t_k} antenna at the k-th tier BS is obtained by applying (19) to (23) as

$$\mathcal{C} \underset{\lambda\to\infty}{\approx} \sum_{k=1}^{\mathcal{T}} \frac{(\lambda\mathcal{A})^{N_{t_k}-1}}{\Gamma(N_{t_k})} \exp(-\lambda\mathcal{A}) \underset{\lambda\longrightarrow\infty}{\longrightarrow} 0 \tag{24}$$

where $\mathcal{A} = \sum_{j=1}^{\mathcal{T}} \frac{\pi r_k^2 \Gamma(1-\delta)\Lambda_j}{\widetilde{P}_j^{-\delta}\beta_k^{-\delta}}$. This last result reveals that, although the SIR increases in multi-antenna ad hoc networks, it will drop to zero as the transmitter density increases.

B. The Impact of the Antenna Size

In this subsection, we consider MISO single-tier networks (i.e., $\mathcal{T} = 1$) in which the BSs are equipped with N_t antennas. We exploit the expressions and tools of the previous sections to derive the scaling laws for different multi-antenna networks including ad hoc, cellular, mmWave and networks with elevated BSs.

1) Antenna Scaling in Ad Hoc Networks: For the multi-antenna case, the coverage expression in (23) can be used to find the asymptotic scaling laws summarized as follows.

Proposition 5: Consider a MISO ad hoc network with N_t transmit antennas such that $\lim_{\lambda\to\infty} \frac{N_t}{\lambda^{\frac{1}{\delta}}} = \gamma$, where $\gamma \in [0, \infty]$, then the asymptotic coverage probability has the following scaling law

$$\lim_{\lambda\to\infty} \mathcal{C} = \begin{cases} 0, & \gamma = 0; \\ \mathrm{H}_{1,1}^{1,0}\left[\frac{T}{\gamma^{\delta}}\middle| \begin{matrix}(1,\delta)\\(0,1)\end{matrix}\right], & \gamma \in \mathbb{R}_+^*; \\ 1, & \gamma = \infty. \end{cases} \tag{25}$$

where $\gamma = 0, \in \mathbb{R}_+^*, \infty$ stands for asymptotically sublinear, linear and super-linear scaling of N_t and $T = \pi r^2 \Gamma(1-\delta)\beta^{\delta}\theta^{\delta}\Lambda$.

Proof: Resorting to the Mellin-Barnes representation of the Fox's H function in (23), it follows that

$$\mathcal{C} \overset{(a)}{=} \frac{1}{2\pi j}\int_{\mathcal{C}} \frac{\Gamma(N_t+\delta s)\Gamma(s)}{\Gamma(N_t)\Gamma(1+\delta s)}(T\lambda)^{-s}\,ds \overset{(b)}{\underset{\lambda\to\infty}{\simeq}} \frac{1}{2\pi j}\int_{\mathcal{C}} \frac{\left(T\frac{\lambda}{N_t^{\delta}}\right)^{-s}}{\Gamma(1+\delta s)}ds, \tag{26}$$

where (a) follows from using [32, Eq. (2.1)] and (b) follows form applying $\lim_{\lambda\to\infty}\frac{\Gamma(N_t+\delta s)}{\Gamma(N_t)} = (N_t)^{\delta s}$. The proof follows by recognizing the Fox's H function definition in [32, Eq. (1.2)], along with its asymptotic expansions near zero [38, Eq. (1.7.14)] and infinity [38, Eq. (1.8.7)].

Hence, based on Proposition 5, we evince that scaling the number of antennas linearly with the density does not prevent the SINR from dropping to zero for high BSs densities (as $\delta^{-1} = \alpha/2$ with $\alpha > 2$) thereby hindering the SINR invariance property. Interestingly, when the number of antennas scales super-linearly with the BSs density, the coverage approaches a finite constant which is desirable since it guarantees a certain quality of service (QoS) for the users in the dense regime.

2) Antenna Scaling in Cellular Networks: Before delving into the analysis, it is important to recall that, in the single antenna case, the coverage probability under a practical bounded path loss model drops to zero as $\lambda \to \infty$ (see Section II.C). In the multi-antenna case, the asymptotic coverage scaling laws are summarized in the following proposition.

Proposition 6: In MISO cellular networks with N_t transmit antennas such that $\lim_{\lambda\to\infty}\frac{N_t}{\lambda} = \zeta$, where $\zeta \in [0,\infty]$, the asymptotic coverage probability under a bounded path loss model has the following scaling law

$$\lim_{\lambda\to\infty}\mathcal{C} = \begin{cases} 0, & \zeta = 0; \\ \mathrm{H}_{1,1}^{1,0}\left[2\pi\frac{\beta}{\eta\zeta}\middle|\begin{matrix}(1,1)\\(0,1)\end{matrix}\right], & \zeta\in\mathbb{R}_+^*; \\ 1, & \zeta=\infty, \end{cases} \tag{27}$$

where $\eta = 2-3\alpha+\alpha^2$ and $\zeta = 0,\in \mathbb{R}_+^*,\infty$ stands for asymptotically sub-linear, linear and super-linear scaling of N_t.

Proof: Due to the intricacy of $\mathcal{L}_I$ in (48), we resort to an analytically tractable tight lower bound. Under the bounded path loss model, the coverage probability in (47) involves the interference Laplace transform $\mathcal{L}_{\mathcal{I}}(s(1+r)^{\alpha}) = \exp(2\pi\lambda\Theta(s(1+r)^{\alpha})$, where we have

$$\begin{aligned}\Theta(s) &= E_g\left[\int_r^{\infty}\left(1-\exp\left(-sg(1+t)^{-\alpha}\right)\right)tdt\right] \\ &\overset{(a)}{\leq} sE[g]\int_r^{\infty} t(1+t)^{-\alpha}dt \\ &\overset{(b)}{\approx} \frac{s}{\eta}\left((1+r)^{1-\alpha}(1-r+\alpha r)\right),\end{aligned} \tag{28}$$

where the inequality in (a) follows from the fact that $1-e^{-x}\leq x$, $\forall x \geq 0$ and (b) holds since g has a unit mean. We note that when r becomes smaller, the inequality in (29) becomes tighter. This is typically the case in ultra-dense networks, where the closest distance to the origin tends to be infinitesimally small. Accordingly, by relabeling $r \leftarrow \frac{r}{\lambda}$, we obtain

$$\Theta\left(s\left(1+\frac{r}{\lambda}\right)^{\alpha}\right) \underset{\lambda\to\infty}{\approx} \frac{s}{\eta}. \tag{29}$$

Hence, the coverage probability can be obtained by merging (29) and (47) as

$$\begin{aligned}\mathcal{C} &\approx \frac{\beta}{\Gamma(N_t)}\int_0^{\infty}\frac{e^{-2\pi\frac{\lambda}{\eta}\xi}}{\xi^2}\mathrm{H}_{1,1}^{0,1}\left[\frac{\xi}{\beta}\middle|\begin{matrix}(2-N_t,1)\\(1,1)\end{matrix}\right]d\xi, \\ &\overset{(a)}{\approx} \frac{1}{\Gamma(N_t)}\mathrm{H}_{1,2}^{2,0}\left[2\pi\frac{\lambda\beta}{\eta}\middle|\begin{matrix}(1,1)\\(0,1),(N_t,1)\end{matrix}\right],\end{aligned} \tag{30}$$

where (a) follows by applying $\int_0^{\infty} f_r(r)dr = 1$ and [32, Eq. (2.3)]. As $N_t(\lambda) \underset{\lambda\to\infty}{\to} \infty$, we obtain

$$C \overset{(b)}{\underset{\lambda\to\infty}{\simeq}} \mathrm{H}_{1,1}^{1,0}\left[2\pi\frac{\lambda\beta}{N_t\eta}\middle|\begin{matrix}(1,1)\\(0,1)\end{matrix}\right], \tag{31}$$

where (b) follows by using an approach similar to (26). The proof follows by resorting to the asymptotic expansions of the Fox's H function in (30) when $\zeta = \frac{N_t}{\lambda}$ is near zero [38, Eq. (1.7.14)] and infinity [38, Eq. (1.8.7)].

The obtained result in (31) allows us to conclude that monotonically increasing the per-user coverage performance by means of ultra-densification is theoretically possible through the deployment of multi-antenna BSs. Specifically, (31) unveils that scaling linearly the number of antennas with the BS density constitutes a solution for avoiding the coverage drop in traditional dense networks.

C. The Impact of Antenna Gain in mmWave Networks

In MISO mmWave networks, the channel gain of the signal g_x follows a gamma distribution $g_x \sim \texttt{Gamma}(N_t, \frac{1}{N_t})$, where N_t is the number of antennas at the BS [27]–[30]. As for the interference received at the typical user, the total channel gain is the product of an arbitrary unit mean small-scale fading gain g [28], [30] and the directional antenna array gain $G(\frac{d}{\lambda_t}\theta_x)$, where d and λ_t are the antenna spacing and wavelength, respectively, and θ_x is a uniformly distributed random variable over $[-1,1]$. An example of antenna pattern based on the cosine function is given by [30], [31]

$$G(x) = \begin{cases} \cos^2\left(\frac{\pi N_t}{2}x\right), & |x| \leq \frac{1}{N_t}; \\ 0, & \text{otherwise.}\end{cases} \tag{32}$$

In dense mmWave network deployments, it is reasonable to assume that the link between any serving BS and the user is in line-of-sight (LOS). Mathematically, the probability of being in a LOS propagation can be formulated as $p(r) = e^{-\tau r}$, where τ is the blockage parameter determined by the density and average size of the spatial blockage [18], [27]. Accordingly, (28) can be derived, based on the cosine antenna pattern and the blockage model, as

$$\begin{aligned}\Theta(s) \leq \frac{\lambda_t s}{\pi d N_t}&\left(\int_r^{\infty} t\frac{e^{-\tau t}}{(1+t)^{\alpha_L}}dt + \int_{(1+r)^{\frac{\alpha_L}{\alpha_N}}-1}^{\infty}\frac{t(1-e^{-\tau t})}{(1+t)^{\alpha_N}}dt\right) \\ &\times\int_0^{\pi}\cos^2\left(\frac{x}{2}\right)dx \\ &\overset{(a)}{\underset{\lambda\to\infty}{=}} \frac{\lambda_t e^{\tau}s}{2dN_t}\left(\mathcal{E}+\mathcal{J}(\tau)\right),\end{aligned} \tag{33}$$

where (a) follows by using the same approach as (29) where $\alpha_L(\alpha_N)$ is the path loss exponent of the LOS (NLOS) link, $\mathcal{E} = \frac{\alpha_N-\alpha_L-1}{(1-\alpha_L)(\alpha_N-2)}$, $\mathcal{J}(\tau) = \frac{(\alpha_L-1+\tau)E_{\alpha_L-1}(\tau)}{\alpha_L-1} - \frac{(\alpha_N-1+\tau)E_{\alpha_N-1}(\tau)}{\alpha_N-1}$, and $E_\nu(\cdot)$ denotes the Exponential Integral function [39]. Then, using (33) and following the same steps as in (30), we obtain

$$\mathcal{C} = \frac{1}{\Gamma(N_t)} \mathrm{H}_{1,2}^{2,0}\left[\frac{\pi\lambda e^{\tau}\beta}{\lambda_t^{-1}d}\left(\mathcal{E}+\mathcal{J}(\tau)\right)\middle| \begin{matrix}(1,1)\\(0,1),(N_t,1)\end{matrix}\right]. \quad (34)$$

Hence, the coverage scaling laws in mmWave networks are given in the following proposition.

Proposition 7: In mmWave networks in which $\lim_{\lambda\to\infty}\lambda_t = 0$, and $\lim_{\lambda\to\infty}\frac{Nt\lambda_t^{-1}}{\lambda} = \rho$, where $\zeta \in [0,\infty]$, the asymptotic coverage probability has the following scaling law

$$\lim_{\lambda\to\infty}\mathcal{C} = \begin{cases} 0, & \rho = 0; \\ \mathrm{H}_{1,1}^{1,0}\left[\pi\frac{\beta e^{\tau}(\mathcal{E}+\mathcal{J}(\tau))}{d\rho}\middle|\begin{matrix}(1,1)\\(0,1)\end{matrix}\right], & \rho\in\mathbb{R}_+^*; \\ 1, & \rho=\infty. \end{cases} \quad (35)$$

Proof: The proof is similar to those of Propositions 5 and 6. The obtained result unveils that the scaling laws derived for mmWave cellular networks are similar to those obtained for legacy frequency bands (see Proposition 6). Specifically, maintaining a linear scaling between the density of BSs and the number of antennas is sufficient to prevent the SINR from dropping to zero and to guarantee a certain quality of service to the UE. In addition, the optimal coverage can be achieved by linearly scaling the number of antennas and the mmWave carrier frequency, which reduces both cost and power consumption. This result provides evidence that moving towards higher frequency bands may be an attractive solution for high capacity ultra-dense networks.

Achieving optimal coverage rely on determining the optimal scaling factor below which further densification becomes destructive or cost-ineffective. This operating point depends on the properties of the channel power distribution and path loss and is of cardinal importance for the successful deployment of ultra-dense networks.

Corollary 1 (Optimal Scaling Factor in Dense mmWave Networks): Capitalizing on Proposition 7, the optimal scaling factor ρ that prevents the outage drop in dense mmWave networks is given by

$$\rho = \frac{N_t f_c}{\lambda} \overset{(a)}{=} \frac{\pi\beta e^{\tau}\left(\mathcal{E}+\mathcal{J}(\tau)\right)}{d}, \quad (36)$$

where f_c is the mmWave carrier frequency and (a) follows from recognizing that $\mathrm{H}_{1,1}^{1,0}\left[x\middle|\begin{matrix}(1,1)\\(0,1)\end{matrix}\right] = U(1-x)$, where $U(x) = \begin{cases}1, & x\geq 0;\\ 0, & \text{otherwise.}\end{cases}$ stands for the Heaviside function [39]. In particular, (36) unveils that under a full-blockage scenario (i.e., $\tau\to\infty$), a super-linear scaling of $N_t f_c$ is required to offset the coverage drop. However, in the no-blockage regime (i.e., $\tau\to 0$), only a linear scaling is needed. Using this framework, enhanced antenna models can be considered to investigate the impact of beam alignment errors on the coverage probability of mmWave dense networks [29].

D. The Impact of Antenna Height in 3D Networks

The vast majority of spatial models for cellular networks are usually 2D and ignore the impact of the BS height. Recent papers have, however, tackled this issue and have highlighted the importance of taking this parameter into account to appropriately estimate the network performance [17]–[19]. In 3D cellular networks, the distance between a BS and the typical UE can be expressed as $\sqrt{h^2+r^2}$, where h is the absolute antenna height difference between the serving BS and the typical UE. Adapting the coverage probability expression in (47) to the 3D context results in an interference distribution whose Laplace transform is of the form $\mathcal{L}_{\mathcal{I}}(s(r^2+h^2)^{\frac{\alpha}{2}}) = \exp(2\pi\lambda\Theta(s(r^2+h^2)^{\frac{\alpha}{2}}))$ where

$$\Theta(s) \leq sE[g]\int_r^{\infty} t(h^2+t^2)^{-\frac{\alpha}{2}}dt \overset{(a)}{=} \frac{s}{\alpha-2}\left(h^2+r^2\right)^{1-\alpha/2}. \quad (37)$$

By employing the change of variable $x \leftarrow \lambda r^2$, we obtain $\mathcal{L}_{\mathcal{I}}\left(s\left(\frac{r}{\lambda}+h^2\right)^{\frac{\alpha}{2}}\right) \underset{\lambda\to\infty}{\approx} e^{\frac{2\pi\lambda s h^2}{\alpha-2}}$. Hence, the coverage probability in 3D multi-antenna cellular networks can be formulated similar to (30) and (31) as

$$\mathcal{C} \underset{\lambda\to\infty}{\simeq} \mathrm{H}_{1,1}^{1,0}\left[2\pi\frac{\lambda h^2\beta}{N_t(\alpha-2)}\middle|\begin{matrix}(1,1)\\(0,1)\end{matrix}\right]. \quad (38)$$

The obtained analytical expression of the coverage probability unveils the impact of the antenna height coupled with other design parameters. Recent works [17]–[19] proposed to maintain the SINR invariance of the coverage probability by lowering the height of the BSs. Based on (38), we evince that the SINR invariance of the coverage probability in 3D networks can be maintained by enforcing a super-linear scaling with the number of antennas.

Corollary 2 (Optimal Scaling Factor in Dense 3D Networks): The optimal scaling factor for the successful deployment of dense 3D networks is

$$\frac{N_t}{\lambda} = \frac{2\pi\beta h^2}{\alpha-2}, \quad (39)$$

which exploits (38) and follows similar to Corollary 1. In particular, the last result shows that the coverage probability monotonically decreases as the BS density increases, if $\lim_{\lambda\to\infty}\frac{Nt}{\lambda} = \zeta\in\mathbb{R}_+^*$, and if $h > \sqrt{\frac{(\alpha-2)\zeta}{2\pi\beta}}$. Interestingly, it is possible to counteract this decay by optimizing the antenna number according to the BS density in order to maintain the per-user coverage performance.

V. Numerical Results

In this section, the obtained analytical frameworks are substantiated with the aid of Monte Carlo simulation using 10^5 independent network realizations. Monte Carlo simulation results are obtained by using the system simulator described in [6], [12], to which the reader is referred for further

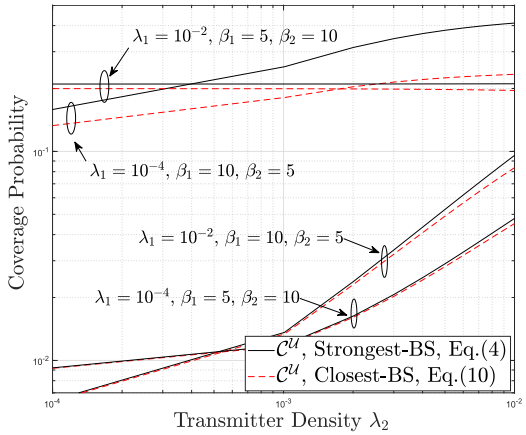

Fig. 1. Coverage probability vs. λ_2 for multi-tier cellular networks with $\mathcal{T} = 2$ over arbitrary Nakagami-m fading with $m_1 = 1.5$, $m_2 = 2.5$, $P_1 = 50$ W, and $P_2 = 1$ W.

information. Unless otherwise stated, the noise power is set to $\sigma^2 = -70$ dBm and the path loss is given by $L(r) = r^{-\alpha}$ for the power-law unbounded model and $L(r) = (1 + r)^{-\alpha}$ for the physically feasible bounded model, with $\alpha = 3$.

The performance comparison between strongest-BS and closest-BS association-based two-tier (i.e., $\mathcal{T} = 2$) cellular networks with unbounded power-law path loss model are illustrated in Fig. 1. Overall, the strongest-BS strategy provides significant performance gain over the closest-BS strategy especially in the low deployment density range. Furthermore, depending on the target SINR thresholds, the effect of increasing the densification of BSs is beneficial while, in some cases, tends to be negligible. Indeed, under the power-law model, the coverage saturates to a non-zero finite constant in the limit of $\lambda_1, \lambda_2 \to \infty$.

Fig. 2 reports the scaling of the coverage probability with the BS densities for both bounded and unbounded path loss models. Analytical and experimental curves are in good agreement. The figure shows that the unbounded model (i.e., $r^{-\alpha}$) guarantees a certain coverage for the users in the dense regime by preventing the SINR from dropping to zero. However, this SINR-invariance property is unattainable because the unbounded model is not sufficiently accurate for short transmission distances. The figure also highlights the diminishing gains achieved with the more realistic bounded path loss model, as anticipated by (17). In this case, new densification strategies are required to prevent the SINR from dropping to zero and avoiding the densification plateau.

Fig. 3 shows the scaling of the SIR coverage probability of ad hoc networks against the transmitter density for various common fading distributions stemming from the general Fox's H fading model. In particular, we corroborate the result of (18) stipulating that increasing the transmitter density degrades the coverage probability, and that the coverage probability can be formulated as the product of an exponential function and a polynomial function of order $\mathcal{T}(m-1)$ of the transmitter density. Moreover, the multi-path fading model has a less noticeable impact on the coverage performance than the path loss model (cf. Fig. 2) and the number of tiers.

Fig. 4 shows the SIR outage probability of cellular networks for an unbounded path loss model versus the antenna size

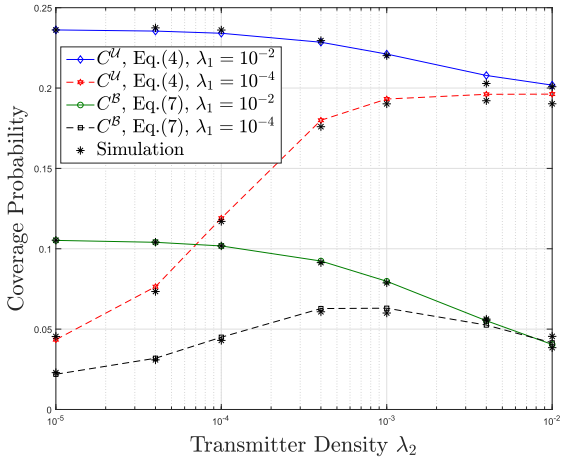

Fig. 2. Coverage probability and scaling laws vs. the BS density λ for multi-tier cellular networks over Nakagami-m fading with $\mathcal{T} = 2$, $P_1 = 50$ W, and $P_2 = 1$ W.

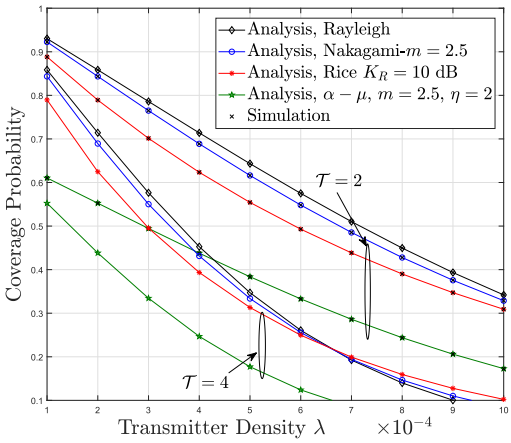

Fig. 3. Coverage probability in ad hoc networks vs. the transmitter density λ when $\beta = 0$ dB.

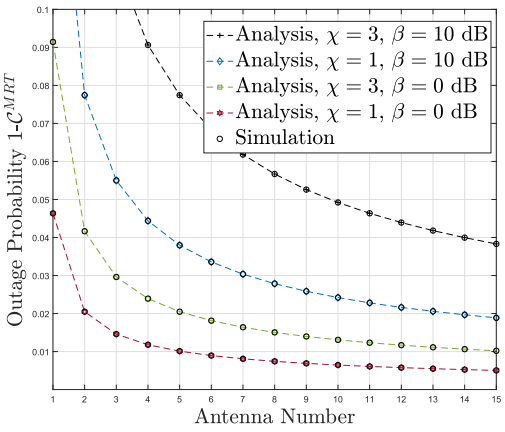

Fig. 4. Outage probability in MISO cellular networks assuming MRT vs. the number of antennas at the transmitter with $\lambda = 10^{-3}$ and $\phi = 1$.

when assuming that the interferers' power gain follows a Gamma distribution, i.e., $g \sim \texttt{Gamma}(\chi, \phi)$. Fig. 4 demonstrates that increasing the antenna size keeps improving the coverage probability, less significantly, however, as the number of antennas grows large.

Fig. 5 illustrates the SIR coverage probability of a two-tiers cellular network over Rician fading with closed-BS

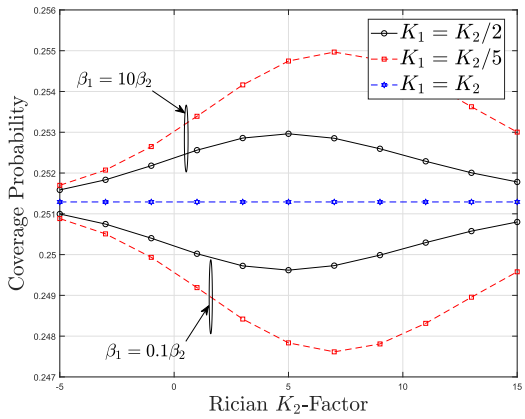

Fig. 5. Coverage probability in a two-tier cellular network under strongest-BS association vs. the Rician K-factor for $\lambda = 10^{-3}$.

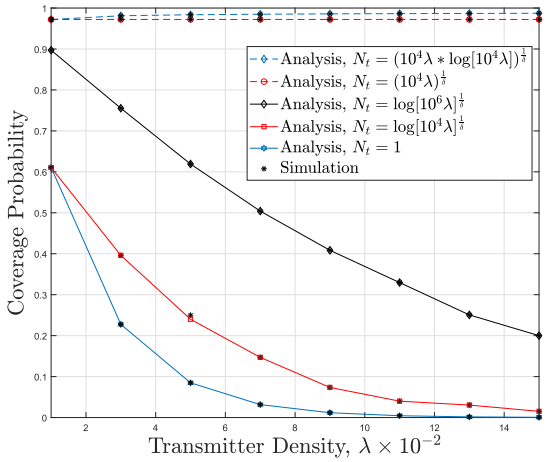

Fig. 6. Coverage probability of MISO ad hoc networks vs the BS density λ for different scaling of the number of antennas.

association obtained from Proposition 3 for different Rician power factors. We observe a substantial increase of the coverage probability only in the non-asymptotic regime, i.e., $K_1 \neq K_2$. Moreover, we observe that the two extreme regimes of pure fading channel with ($K \rightarrow 0$) and pure LOS propagation ($K \rightarrow \infty$) achieve worse coverage performance.

Fig. 6 shows the scaling of the coverage probability in ad hoc networks against the transmitter density for different scaling rates of the number of antennas: super-linear, linear, sub-linear, and constant (i.e, single antenna). We note that the coverage decreases with the density as compared with the single antenna case, as anticipated in (24), and also when the number of antennas is scaled sublinearly or linearly with the density, as predicted by Proposition 5. We observe that a super-linear scaling of the number of antennas with the BS density is required to prevent the SIR from dropping to zero, and thereby restore the SIR invariance property.

The impact of the BS height on the coverage probability is illustrated in Fig. 7. As predicted in Section IV.D, we note that a linear scaling of the number of antennas is required to maintain a non-zero SINR for low values of h. When the BS height increases, the coverage probability decreases due to the increase of the path loss and the linear scaling becomes insufficient.

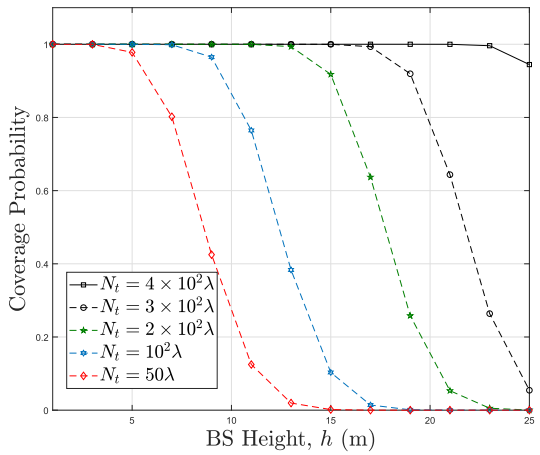

Fig. 7. Coverage probability of MISO cellular networks vs the BS height h for different scaling of the antenna number N_t.

VI. Conclusion

By leveraging the properties of Fox's H random variables, we developed a unifying framework to characterize the coverage probability of heterogeneous and muti-antenna networks under both the closest-BS and the strongest-BS cell association strategies. We studied the impact of BS densification on the coverage performance both under bounded and unbounded path loss models. By direct inspection of the obtained analytical framework, we have been able to derive exact closed-form formulations and scaling laws of the coverage probability for two typical network models, i.e., heterogeneous and multi-antenna cellular and ad hoc networks, while incorporating generalized fading distributions. The obtained results encompass insightful relationships between the BS density and the relative antenna array size, gain and height, showing how the coverage can be maintained whilst increasing the network density. The insights provided in this work are of cardinal importance for optimally deploying general ultra-dense networks.

VII. Appendix A: Proof of Proposition 1

With the closest-BS association strategy, the coverage probability is given by

$$\mathcal{C} \triangleq \sum_{k=1}^{\mathcal{T}} \theta_k \mathbb{P}\left(\text{SINR}_k > \beta_k\right) = \sum_{k=1}^{\mathcal{T}} \theta_k \mathbb{E}_{r_k}\left\{\mathcal{C}(r_k)\right\}, \quad (40)$$

where θ_k denotes the association probability and is expressed as $\theta_k = \frac{\lambda_k}{\sum_{j\in\mathcal{T}} \lambda_j \widetilde{P}_j^{\delta}}$, and $\widetilde{P}_j = \frac{P_j}{P_k}$. Using [10, Theorem 1] and [11, Eq. (39)] and applying the Fox's H transform in [32, Eq. (2.3)], the coverage probability under unbounded path loss model, denoted as $\mathcal{C}^{\mathcal{U}}$, is given by

$$\mathcal{C}^{\mathcal{U}}(r_k) = \int_0^{\infty} \frac{1}{\sqrt{\xi}} \mathcal{L}^{-1}\left\{\frac{1}{\sqrt{s}} \mathrm{H}_{p,q}^{u,v}\left\{f(t);\mathcal{P}\right\}(s\xi); s; \beta_k\right\} \times e^{-\sigma^2 \xi \frac{r_k^{\alpha}}{P_k}} \prod_{j\in\mathcal{T}} \mathcal{L}_{\mathcal{I}_j}\left(\xi \frac{r_k^{\alpha}}{P_k}\right) d\xi, \quad (41)$$

where $f(t) = \sqrt{t}\mathcal{J}_1\left(2\sqrt{st\xi}\right)$, $\mathrm{H}_{p,q}^{u,v}\left\{f(t);\mathcal{P}\right\}(s)$ is the Mellin transform [32, Eq. (2.3)], $\mathcal{J}_1(x) = \mathrm{H}_{0,2}^{1,0}\left(\frac{x^2}{4}; (1,1,\frac{1}{2},-\frac{1}{2},1,1)\right)$ is the Bessel function of

the first kind [39, Eq. (8.402)], and $\mathcal{L}^{-1}$ is the inverse Laplace transform. Moreover $\mathcal{L}_{\mathcal{I}_j}$, in (47), is the Laplace transform of the aggregate interference from the j-th tier evaluated as

$$\mathcal{L}_{\mathcal{I}_j}(s) = \exp(2\pi\lambda_j \Theta(s)), \tag{42}$$

where

$$\begin{aligned}\Theta\mid_{g=y}(s) &\overset{(a)}{=} \int_{\left(\frac{P_j}{P_k}\right)^{\frac{2}{\alpha}} r_k}^{\infty} \left(1-\exp\left(-syP_j r^{-\alpha}\right)\right) rdr \\ &\overset{(b)}{=} \frac{syP_j}{\alpha}\int_{\frac{P_k}{P_j} r_k^{-\alpha}}^{\infty} x^{-\frac{2}{\alpha}} e^{-syx}\,{}_1\mathrm{F}_1(1,2,syx)\,dx \\ &\overset{(c)}{=} \frac{sy\widetilde{P}_j^{\delta-1}P_j}{r^{\alpha-2}(2-\alpha)}\,{}_2\mathrm{F}_2\left(1,-\frac{2}{\alpha}+1;2;-\frac{2}{\alpha}+2;-\frac{syP_k}{r_k^{\alpha}}\right),\end{aligned} \tag{43}$$

where (a) follows from the probability generating functional [9], [40], while relabeling x as $r_k^{-\alpha}$ and $(1-e^{-x})/x = e^{-x}\,{}_1\mathrm{F}_1(1,2;x)$ is applied in (b), and (c) follows from applying $\int x^{\beta-1}e^{-cx}\,{}_1\mathrm{F}_1(a,b,cx)dx = \frac{x^{\beta}}{\beta}\,{}_2\mathrm{F}_2(b-a,\beta,b,\beta+1,-cx)$. Hence, we obtain

$$\begin{aligned}\mathcal{L}_{\mathcal{I}_j}(\xi) &= \exp(-2\pi\lambda_j \mathbb{E}_g[\Theta(s)]) \\ &= \exp\left(-\pi\delta\lambda_j \widetilde{P}_j^{\delta-1}\frac{\xi r_k^{2-\alpha}P_j}{(1-\delta)}\mathrm{H}_{p,q}^{u,v}\left\{h(t);\mathcal{P}\right\}(\xi)\right),\end{aligned} \tag{44}$$

where $\delta = \frac{2}{\alpha}$, $h(t) = t\;{}_2\mathrm{F}_2\left(1,1-\delta;2;2-\delta;-\xi t r_k^{-\alpha}\right) = t\mathrm{H}_{2,3}^{1,2}(t;\mathcal{P}_1)$, $\mathcal{P}_1 = (1-\delta,\xi(r_k^2)^{-\frac{\alpha}{2}},(0,\delta),(0,-1,\delta-1),\mathbf{1}_2,\mathbf{1}_3)$, and ${}_{\mathrm{p}}\mathrm{F}_{\mathrm{q}}(\cdot)$ is the generalized hypergeometric function of [39, Eq. (9.14.1)]. In (44), in particular, we first take the expectation over the interferers' locations and then average over the Fox's H distributed channel gains, which is in the reverse order compared to the conventional derivations in [4]–[9]. The reason behind this order swapping is that the Fox's H fading model is more complicated than the conventional exponential model, and therefore averaging over it in a latter step preserves the analytical tractability.

Finally, applying [32, Eq. (1.58)], the Mellin transform [32, Eq. (2.3)], and the inverse Laplace transform of the Fox's H function [32, Eq. (2.21)] given by

$$\mathcal{L}^{-1}\{x^{-\rho}\mathrm{H}_{p,q}^{u,v}(x;\mathcal{P});x;t\} = t^{-\rho-1}\mathrm{H}_{p+1,q}^{u,v}\left(\frac{1}{t};\mathcal{P}_l\right), \tag{45}$$

where $\mathcal{P}_l = (\kappa,c,(a,\rho),b,(A,1),B)$, the desired result is obtained after applying the Fox's H reduction formulae in [32, Eq. (1.57)]. The coverage probability over Fox's H fading[5] for a receiver connecting to a k-th tier BS located at x_k is given by

$$\begin{aligned}\mathcal{C}^{\mathcal{U}}(r_k) = \int_0^{\infty}\frac{1}{\xi^2}\mathrm{H}_{q,p+1}^{v,u}\left(\xi;\mathcal{P}_{\mathcal{U}}^k\right)e^{-\sigma^2\xi\frac{r_k^{\alpha}}{P_k}} \\ \exp\left(-\pi\delta\sum_{j\in\mathcal{T}} r_k^2\lambda_j\widetilde{P}_j^{\delta}\xi\mathrm{H}_{q+2,p+3}^{v+1,u+2}\left(\xi;\mathcal{P}_{\mathcal{U}}^{\mathcal{I}}\right)\right)d\xi,\end{aligned} \tag{46}$$

[5]We dropped the index i from Fox's H distribution $\{\mathcal{O}_i,\mathcal{P}_i\}$ for notation simplicity.

where $\widetilde{P}_j = \frac{P_j}{P_k}$, $\delta = \frac{2}{\alpha}$, and the parameter sequences $\mathcal{P}_{\mathcal{U}}^k = \left(\kappa\beta_k,\frac{1}{c\beta_k},1-b,(1-a,1),\mathcal{B},(A,1)\right)$, and $\mathcal{P}_{\mathcal{U}}^{\mathcal{I}} = \Big(\frac{\kappa}{c^2},\frac{1}{c},(1-b-2B,0,\delta),(0,1-a-2A,-1,\delta-1),(\mathcal{B},1,1),(1,A,1,1)\Big)$. Recall that the pdf of the link's distance r_k is given by $f_{r_k}(x) = \frac{2\pi\lambda_k}{\theta_k}x\exp\left(-\sum_{j\in\mathcal{T}}\pi x^2\lambda_j\widetilde{P}_j^{\delta}\right)$ [3], [40]. Then recognizing that $\exp(-x) = \mathrm{H}_{0,1}^{1,0}(x;1,1,0,1,1,1)$ [32, Eq. (1.125)] in (46), we apply [32, Eq. (2.3)] to obtain the average coverage probability in (4) after some manipulations.

VIII. Appendix B: Proof of Proposition 2

The proof of Proposition 2 relies on the same approach adopted in Appendix A, yielding

$$\begin{aligned}\mathcal{C}^{\mathcal{B}}(r_k) = \int_0^{\infty}\frac{1}{\sqrt{\xi}}\,\mathcal{L}^{-1}\left\{\frac{1}{\sqrt{s}}\mathrm{H}_{p,q}^{u,v}\left\{f(t);\mathcal{P}\right\}(s\xi);s;\beta_k\right\} \\ \times e^{-\sigma^2\xi\frac{(1+r_k)^{\alpha}}{P_k}}\prod_{j\in\mathcal{T}}\mathcal{L}_{\mathcal{I}_j}\left(\xi\frac{(1+r_k)^{\alpha}}{P_k}\right)d\xi,\end{aligned} \tag{47}$$

where rearranging [11, Eq. (39)] after carrying out the change of variable relabeling $(1+x)^{-\alpha}$ as x, we have

$$\begin{aligned}\mathcal{L}_{\mathcal{I}_j}(\xi) = \exp\Bigg(-\pi\delta\lambda_j\xi\widetilde{P}_j^{\delta-1}\Bigg(\frac{(1+r_k)^{2-\alpha}P_j}{(1-\delta)}\mathrm{H}_{p,q}^{u,v}\{h_1(t);\mathcal{P}_1\}(\xi) \\ -\frac{(1+r_k)^{1-\alpha}P_j}{\left(1-\frac{\delta}{2}\right)}\mathrm{H}_{p,q}^{u,v}\left\{h_2(t);\mathcal{P}\right\}(\xi)\Bigg)\Bigg),\end{aligned} \tag{48}$$

where $h_1(t) = t\;{}_2\mathrm{F}_2\left(1,1-\delta;2;2-\delta;-\xi t(1+r_k)^{-\alpha}\right)$ and $h_2(t) = t\;{}_2\mathrm{F}_2\left(1,1-\frac{\delta}{2};2;2-\frac{\delta}{2};-\xi t(1+r_k)^{-\alpha}\right)$. Finally applying the Mellin transform in [32, Eq. (2.3)] and plugging the obtained result into (47), the coverage probability under bounded path loss model is obtained as

$$\begin{aligned}\mathcal{C}^{\mathcal{B}}(r_k) = \int_0^{\infty}\frac{1}{\xi^2}\mathrm{H}_{q,p+1}^{n,m}\left(\xi,\mathcal{P}_{\mathcal{B}}^k\right)\exp\Bigg(-\frac{\sigma^2}{P_k}\xi(1+r_k)^{\alpha} \\ -\sum_{j\in\mathcal{M}}\pi\lambda_j\widetilde{P}_j^{\delta}\delta\xi\Bigg((1+r_k)^2\mathrm{H}_{q+2,p+3}^{n+1,m+2}\left(\xi,\mathcal{P}_{\mathcal{B}}^{1,\mathcal{I}}\right) \\ -(1+r_k)\mathrm{H}_{q+2,p+3}^{n+1,m+2}\left(\xi,\mathcal{P}_{\mathcal{B}}^{2,\mathcal{I}}\right)\Bigg)\Bigg)d\xi,\end{aligned} \tag{49}$$

where $\mathcal{P}_{\mathcal{B}}^k = \mathcal{P}_{\mathcal{U}}^k$, $\mathcal{P}_{\mathcal{B}}^{1,\mathcal{I}} = \left(\frac{\kappa}{c^2},\frac{1}{c},(1-b-2B,0,\delta),(0,1-a-2A,-1,\delta-1),(\mathcal{B},1,1),(1,A,1,1)\right)$, and $\mathcal{P}_{\mathcal{B}}^{2,\mathcal{I}} = \left(\frac{\kappa}{c^2},\frac{1}{c},\left(1-b-2B,0,\frac{\delta}{2}\right),\left(0,1-a-2A,-1,\frac{\delta}{2}-1\right),(\mathcal{B},1,1),(1,A,1,1)\right)$. Recalling that $\mathcal{C}^{\mathcal{B}} = \sum_{k=1}^{\mathcal{T}}\theta_k\mathbb{E}_{r_k}\left\{\mathcal{C}^{\mathcal{B}}(r_k)\right\}$, then as inferred from (49), the coverage probability for bounded path loss model is obtained as a function of a two-fold multiple integral. Due to space limitations, the details are omitted. However, in the special case when $\sigma^2 = 0$ (i.e., interference-limited scenario), Proposition 2 follows by averaging (49) over r_k along with some manipulations similar to Proposition 1.

IX. Appendix C: Proof of Proposition 3

Based on [11], the Laplace transform of the aggregate interference from tier j under the max-SINR association strategy is evaluated as $\mathcal{L}_{\mathcal{I}_j}(\xi) = \exp\left(-\pi\lambda_j\xi^{\delta}\Gamma\left(1-\delta\right)\mathbb{E}[g^{\delta}]\right)$, where $\mathbb{E}[g^{\delta}]$ is the Mellin transform of the Fox's H function obtained as $\mathbb{E}[g^{\delta}] = \Lambda$ [32, Eq. (2.8)]. According to [9, Lemma 1], the coverage probability under strongest-BS association is

$$\mathcal{C} = 2\pi \sum_{k\in\mathcal{M}} \lambda_k \int_0^{\infty} r_k \mathcal{C}(r_k) d_{r_k}, \tag{50}$$

where, following the analytical steps as in Appendix A, we obtain

$$\begin{aligned}\mathcal{C} \;&=\; 2\pi \sum_{k\in\mathcal{T}} \lambda_k \int_0^{\infty} r_k \int_0^{\infty} \frac{1}{\xi^2} \mathrm{H}_{q,p+1}^{v,u}\left(\xi; \mathcal{P}_{\mathcal{U}}^{k}\right) \\ &\quad \exp\left(-\sum_{j\in\mathcal{T}} r_k^2 \pi \lambda_j \widetilde{P}_j^{\delta} \xi^{\delta} \Gamma(1-\delta)\Lambda_j\right) d\xi dr_k \\ &\overset{(a)}{=}\; 2\pi \sum_{k\in\mathcal{T}} \frac{\lambda_k}{\delta} \int_0^{\infty} r_k \int_0^{\infty} \frac{1}{\xi^2} \mathrm{H}_{q,p+1}^{v,u}\left(\xi; \mathcal{P}_{\mathcal{U}}^{k}\right) \\ &\mathrm{H}_{0,1}^{1,0}\left(\left(\sum_{j\in\mathcal{T}} r_k^2 \pi \lambda_j \widetilde{P}_j^{\delta} \Gamma(1-\delta)\Lambda_j\right)^{\frac{1}{\delta}} \xi; \left(1,1,1,0,1,\frac{1}{\delta}\right)\right) d\xi dr_k,\end{aligned} \tag{51}$$

where (a) follows from substituting $\exp(-x) = \mathrm{H}_{0,1}^{1,0}(x; 1,1,-,0,-,1)$ [32, Eq. (1.125)] and applying the transformation $\mathrm{H}_{p,q}^{u,v}\left[x\middle|\begin{matrix}(a_i, kA_j)_p \\ (b_i, kB_j)_q\end{matrix}\right] = \frac{1}{k}\mathrm{H}_{p,q}^{u,v}\left[x^{\frac{1}{k}}\middle|\begin{matrix}(a_i, A_j)_p \\ (b_i, B_j)_q\end{matrix}\right]$. Finally, applying [32, Eq. (2.3)] to evaluate the inner-integral in (51), yields the strongest-BS based coverage probability as shwon in Proposition 3.

References

[1] I. Trigui, S. Affes, M. Di Renzo, and D. N. K. Jayakody, "SINR coverage analysis of dense HetNets over fox's H-fading channels," in *Proc. IEEE Wireless Commun. Netw. Conf. (WCNC)*, Seoul, South Korea, Apr. 2020, pp. 1–6.

[2] J. G. Andrews *et al.*, "What will 5G be?" *IEEE J. Sel. Areas Commun.*, vol. 32, no. 6, pp. 1065–1082, Jun. 2014.

[3] C. Li, J. Zhang, J. G. Andrews, and K. B. Letaief, "Success probability and area spectral efficiency in multiuser MIMO HetNets," *IEEE Trans. Commun.*, vol. 64, no. 4, pp. 1544–1556, Apr. 2016.

[4] J. G. Andrews, F. Baccelli, and R. K. Ganti, "A tractable approach to coverage and rate in cellular networks," *IEEE Trans. Commun.*, vol. 59, no. 11, pp. 3122–3134, Nov. 2011.

[5] M. Di Renzo and P. Guan, "Stochastic geometry modeling of coverage and rate of cellular networks using the Gil-Pelaez inversion theorem," *IEEE Commun. Lett.*, vol. 18, no. 9, pp. 1575–1578, Sep. 2014.

[6] M. Di Renzo, A. Guidotti, and G. E. Corazza, "Average rate of downlink heterogeneous cellular networks over generalized fading channels: A stochastic geometry approach," *IEEE Trans. Commun.*, vol. 61, no. 7, pp. 3050–3071, Jul. 2013.

[7] Y. J. Chun, S. L. Cotton, H. S. Dhillon, A. Ghrayeb, and M. O. Hasna, "A stochastic geometric analysis of device-to-device communications operating over generalized fading channels," *IEEE Trans. Wireless Commun.*, vol. 16, no. 7, pp. 4151–4165, Jul. 2017.

[8] A. K. Gupta, H. S. Dhillon, S. Vishwanath, and J. G. Andrews, "Downlink multi-antenna heterogeneous cellular network with load balancing," *IEEE Trans. Commun.*, vol. 62, no. 11, pp. 4052–4067, Nov. 2014.

[9] H. S. Dhillon, R. K. Ganti, F. Baccelli, and J. G. Andrews, "Modeling and analysis of K-tier downlink heterogeneous cellular networks," *IEEE J. Sel. Areas Commun.*, vol. 30, no. 3, pp. 550–560, Apr. 2012.

[10] I. Trigui, S. Affes, and B. Liang, "Unified stochastic geometry modeling and analysis of cellular networks in LOS/NLOS and shadowed fading," *IEEE Trans. Commun.*, vol. 65, no. 12, pp. 5470–5486, Dec. 2017.

[11] I. Trigui and S. Affes, "Unified analysis and optimization of D2D communications in cellular networks over fading channels," *IEEE Trans. Commun.*, vol. 67, no. 1, pp. 724–736, Jan. 2019.

[12] M. Di Renzo, W. Lu, and P. Guan, "The intensity matching approach: A tractable stochastic geometry approximation to system-level analysis of cellular networks," *IEEE Trans. Wireless Commun.*, vol. 15, no. 9, pp. 5963–5983, Sep. 2016.

[13] M. Di Renzo and P. Guan, "A mathematical framework to the computation of the error probability of downlink MIMO cellular networks by using stochastic geometry," *IEEE Trans. Commun.*, vol. 62, no. 8, pp. 2860–2879, Aug. 2014.

[14] M. G. Khoshkholgh and V. C. M. Leung, "Coverage analysis of max-SIR cell association in HetNets under nakagami fading," *IEEE Trans. Veh. Technol.*, vol. 67, no. 3, pp. 2420–2438, Mar. 2018.

[15] J. Liu, M. Sheng, L. Liu, and J. Li, "Effect of densification on cellular network performance with bounded pathloss model," *IEEE Commun. Lett.*, vol. 21, no. 2, pp. 346–349, Feb. 2017.

[16] V. M. Nguyen and M. Kountouris, "Performance limits of network densification," *IEEE J. Sel. Areas Commun.*, vol. 35, no. 6, pp. 1294–1308, Jun. 2017.

[17] M. Ding, P. Wang, D. López-Pérez, G. Mao, and Z. Lin, "Performance impact of LoS and NLoS transmissions in dense cellular networks," *IEEE Trans. Wireless Commun.*, vol. 15, no. 3, pp. 2365–2380, Mar. 2016.

[18] I. Atzeni, J. Arnau, and M. Kountouris, "Downlink cellular network analysis with LOS/NLOS propagation and elevated base stations," *IEEE Trans. Wireless Commun.*, vol. 17, no. 1, pp. 142–156, Jan. 2018.

[19] M. Filo, C. H. Foh, S. Vahid, and R. Tafazolli, "Stochastic geometry analysis of ultra-dense networks: Impact of antenna height and performance limits," 2017, *arXiv:1712.02235*. [Online]. Available: http://arxiv.org/abs/1712.02235

[20] N. Lee, R. W. Heath, Jr., and F. Baccelli, "Spectral efficiency scaling laws in dense random wireless networks with multiple receive antennas," *IEEE Trans. Inf. Theory*, vol. 62, no. 3, pp. 1344–1359, Mar. 2016.

[21] H. ElSawy, A. Sultan-Salem, M.-S. Alouini, and M. Z. Win, "Modeling and analysis of cellular networks using stochastic geometry: A tutorial," *IEEE Commun. Surveys Tuts.*, vol. 19, no. 1, pp. 167–203, 1st Quart., 2017.

[22] X. Zhang and J. G. Andrews, "Downlink cellular network analysis with multi-slope path loss models," *IEEE Trans. Commun.*, vol. 63, no. 5, pp. 1881–1894, May 2015.

[23] R. K. Ganti and M. Haenggi, "Asymptotics and approximation of the SIR distribution in general cellular networks," *IEEE Trans. Wireless Commun.*, vol. 15, no. 3, pp. 2130–2143, Mar. 2016.

[24] V. Chandrasekhar, M. Kountouris, and J. G. Andrews, "Coverage in multi-antenna two-tier networks," *IEEE Trans. Wireless Commun.*, vol. 8, no. 10, pp. 5314–5327, Oct. 2009.

[25] A. M. Hunter, J. G. Andrews, and S. Weber, "Transmission capacity of ad hoc networks with spatial diversity," *IEEE Trans. Wireless Commun.*, vol. 7, no. 12, pp. 5058–5071, Dec. 2008.

[26] G. George, R. K. Mungara, A. Lozano, and M. Haenggi, "Ergodic spectral efficiency in MIMO cellular networks," *IEEE Trans. Wireless Commun.*, vol. 16, no. 5, pp. 2835–2849, May 2017.

[27] X. Yu, C. Li, J. Zhang, M. Haenggi, and K. B. Letaief, "A unified framework for the tractable analysis of multi-antenna wireless networks," *IEEE Trans. Wireless Commun.*, vol. 17, no. 12, pp. 7965–7980, Dec. 2018.

[28] M. Di Renzo and P. Guan, "Stochastic geometry modeling and system-level analysis of uplink heterogeneous cellular networks with multi-antenna base stations," *IEEE Trans. Commun.*, vol. 64, no. 6, pp. 2453–2476, Jun. 2016.

[29] M. Cheng, J.-B. Wang, Y. Wu, X.-G. Xia, K.-K. Wong, and M. Lin, "Coverage analysis for millimeter wave cellular networks with imperfect beam alignment," *IEEE Trans. Veh. Technol.*, vol. 67, no. 9, pp. 8302–8314, Sep. 2018.

[30] X. Yu, J. Zhang, M. Haenggi, and K. B. Letaief, "Coverage analysis for millimeter wave networks: The impact of directional antenna arrays," *IEEE J. Sel. Areas Commun.*, vol. 35, no. 7, pp. 1498–1512, Jul. 2017.

[31] N. Deng, M. Haenggi, and Y. Sun, "Millimeter-wave device-to-device networks with heterogeneous antenna arrays," *IEEE Trans. Commun.*, vol. 66, no. 9, pp. 4271–4285, Sep. 2018.

[32] A. M. Mathai, R. K. Saxena, and H. J. Haubol, *The H-Function: Theory and Applications*. New York, NY, USA: Springer, 2010.

[33] S. K. Yoo, S. L. Cotton, P. C. Sofotasios, M. Matthaiou, M. Valkama, and G. K. Karagiannidis, "The Fisher–Snedecor $\mathcal{F}$ distribution: A simple and accurate composite fading model," *IEEE Commun. Lett.*, vol. 21, no. 7, pp. 1661–1664, Jul. 2017.
[34] F. Yilmaz and M.-S. Alouini, "A novel unified expression for the capacity and bit error probability of wireless communication systems over generalized fading channels," *IEEE Trans. Commun.*, vol. 60, no. 7, pp. 1862–1876, Jul. 2012.
[35] Y. Jeong, H. Shin, and M. Z. Win, "H-transforms for wireless communication," *IEEE Trans. Inf. Theory*, vol. 61, no. 7, pp. 3773–3809, Jul. 2015.
[36] M. Di Renzo and W. Lu, "System-level analysis and optimization of cellular networks with simultaneous wireless information and power transfer: Stochastic geometry modeling," *IEEE Trans. Veh. Technol.*, vol. 66, no. 3, pp. 2251–2275, Mar. 2017.
[37] M. Di Renzo, S. Wang, and X. Xi, "Inhomogeneous double thinning—Modeling and analysis of cellular networks by using inhomogeneous Poisson point processes," *IEEE Trans. Wireless Commun.*, vol. 17, no. 8, pp. 5162–5182, Aug. 2018.
[38] A. Kilbas and M. Saigo, *H-Transforms: Theory and Applications*. Boca Raton, FL, USA: CRC Press, 2004.
[39] I. S. Gradshteyn and I. M. Ryzhik, *Table of Integrals, Series and Products*, 5th ed. New York, NY, USA: Academic, 1994.
[40] M. Haenggi, *Stochastic Geometry for Wireless Networks*. Cambridge, U.K.: Cambridge Univ. Press, 2012.

Imène Trigui (Member, IEEE) received the M.Sc. and Ph.D. degrees (Hons.) from the National Institute of Scientific Research (INRS-EMT), University of Quebec, Montreal, QC, Canada, in May 2010 and August 2015, respectively. From 2016 to 2018, she was a Post-Doctoral Research Fellow with the Department of Electrical Engineering, Toronto University, Toronto, ON, Canada. From 2018 to 2019, she was a Research Scientist with INRS-EMT, University of Quebec. Since 2020, she has been a RESMIQ Post-Doctoral Fellow with the University of Québec at Montréal. In recognition of her academic, research, and scholarly achievements, she was a recipient of several major awards, including the Natural Sciences and Engineering Research Council of Canada (NSERC) Postdoctoral Fellowship from 2016 to 2018 and the top-tier Alexander-Graham-Bell Canada Graduate Scholarship from the National Sciences and Engineering Research Council from 2012 to 2014. She also received the Best Paper Award from IEEE VTC'2010-Fall. She serves regularly as a reviewer for many top international journals and conferences in her field.

Sofiène Affes (Senior Member, IEEE) received the Diplome d'Ingénieur in telecommunications and the Ph.D. degree (Hons.) in signal processing from Télécom ParisTech (ENST), Paris, France, in 1992 and 1995, respectively. He was a Research Associate with INRS, Montreal, QC, Canada, till 1997, an Assistant Professor till 2000, and an Associate Professor till 2009. He is currently a Full Professor and the Director of PERWADE, a unique M4 million research-training program on wireless in Canada involving 27 partners from 8 universities and 10 industrial organizations. He currently serves as a member on the Editorial Board for the *Sensors* Journal (MDPI) and the Advisory Board for the *Journal of Multidisciplinary Sciences* (MDPI). He has been twice a recipient of the Discovery Accelerator Supplement Award from NSERC, from 2008 to 2011 and from 2013 to 2016. In 2008 and 2015, he received the IEEE VTC Chair Recognition Award from IEEE VTS and the IEEE ICUWB Chair Recognition Certificate from IEEE MTT-S for exemplary contributions to the success of both events, respectively. From 2003 to 2013, he was the Canada Research Chair of Wireless Communications. Since October 2017, he holds a Cyrille-Duquet Research Chair of Telecommunications. In 2006, 2015, and 2017, he served as a General Co-Chair or the Chair of IEEE VTC'2006-Fall, IEEE ICUWB'2015, and IEEE PIMRC'2017, all held in Montreal, QC, Canada. He previously served as an Associate Editor for the IEEE TRANSACTIONS ON WIRELESS COMMUNICATIONS, the IEEE TRANSACTIONS ON COMMUNICATIONS, the IEEE TRANSACTIONS ON SIGNAL PROCESSING, the *Journal of Electrical and Computer Engineering* (Hindawi), and the *Journal of Wireless Communications and Mobile Computing* (Wiley).

Marco Di Renzo (Fellow, IEEE) received the Laurea *(cum laude)* and Ph.D. degrees in electrical engineering from the University of L'Aquila, Italy, in 2003 and 2007, respectively, and the Habilitation à Diriger des Recherches (Doctor of Science) degree from University Paris-Sud, France, in 2013. Since 2010, he has been with the French National Center for Scientific Research (CNRS), where he is a CNRS Research Director (CNRS Professor) with the Laboratory of Signals and Systems (L2S), Paris-Saclay University-CNRS and CentraleSupelec, Paris, France. In Paris-Saclay University, he serves as the Coordinator of the Communications and Networks Research Area with the Laboratory of Excellence DigiCosme, and as a member of the Admission and Evaluation Committee with the Ph.D. School on Information and Communication Technologies. He is a Highly Cited Researcher (Clarivate Analytics, Web of Science), a World's Top 2% Scientist from Stanford University, and a Fellow of the IET. He has received several individual distinctions and research awards, which include the IEEE Communications Society Best Young Researcher Award for Europe, Middle East, and Africa, the Royal Academy of Engineering Distinguished Visiting Fellowship, the IEEE Jack Neubauer Memorial Best System Paper Award, the IEEE Communications Society Young Professional in Academia Award, the SEE-IEEE Alain Glavieux Award, and the 2019 IEEE ICC Best Paper Award. In 2019, he was a recipient of the Nokia Foundation Visiting Professorship for conducting research on metamaterial-assisted wireless communications at Aalto University, Finland. He currently serves as the Editor-in-Chief for IEEE COMMUNICATIONS LETTERS and a Distinguished Speaker for the IEEE VEHICULAR TECHNOLOGY SOCIETY. From 2017 to 2020, he was a Distinguished Lecturer with the IEEE VEHICULAR TECHNOLOGY SOCIETY and IEEE COMMUNICATIONS SOCIETY. He served as an Editor and an Associate Editor-in-Chief for IEEE COMMUNICATIONS LETTERS, and as an Editor for IEEE TRANSACTIONS ON COMMUNICATIONS and IEEE TRANSACTIONS ON WIRELESS COMMUNICATIONS. He also serves as the Founding Chair for the Special Interest Group on Reconfigurable Intelligent Surfaces of the Wireless Technical Committee, IEEE Communications Society. He is also the Founding Lead Editor for the IEEE Communications Society Best Readings in Reconfigurable Intelligent Surfaces.

Dushantha Nalin K. Jayakody (Senior Member, IEEE) received the M.Sc. degree in electronics and communications engineering from the Department of Electrical and Electronics Engineering, Eastern Mediterranean University, Turkey (under the University full graduate scholarship), and the Ph.D. degree in electronics and communications engineering from the University College Dublin, Ireland. From 2014 to 2016, he was a Post-Doctoral Research Fellow with the University of Tartu, Estonia, and the University of Bergen, Norway. Since 2016, he has been a Professor with the School of Computer Science and Robotics, National Research Tomsk Polytechnic University (TPU), Russia. He also serves as the Head of Research and Educational Center on Automation and Information Technologies and the Founder of the Tomsk Infocomm Laboratory, TPU. Since 2019, he has been serves as the Head of the School of Postgraduate and Research, Sri Lanka Technological Campus (SLTC), Padukka, Sri Lanka, and the Founding Director of the Centre of Telecommunication Research, SLTC. He held visiting and/or sabbatical positions with the Centre for Telecommunications Research, University of Sydney, Australia, in 2015, and Texas A&M University in 2018. He is supervising/supervised 11 Ph.D. students and many masters and undergraduate students. In his career, so far, he has attracted nearly $6M$ research funding. He has organized or co-organized more than 25 workshops and special sessions of various IEEE conferences. He has published over 180 international peer-reviewed journal and conference papers and books. His research interests include PHY and NET layer prospective of 5G communications technologies, such as NOMA for 5G, cooperative wireless communications, device to device communications, LDPC codes, and unmanned ariel vehicle. He is a Fellow of IET. He has received the Best Paper Award from the IEEE International Conference on Communication, Management and Information Technology (ICCMIT) in 2017 and the International Conference on Emerging Technologies of Information and Communications, Bhutan, in March 2019, the Education Leadership Award from the World Academic Congress in July 2019, the Outstanding Faculty Award from National Research Tomsk Polytechnic University, Russia, in 2017 and 2018, and the Distinguished Researcher Award in Wireless Communications, Chennai, India, in 2019. He served as the Chair, a Session Chair, or a Technical Program Committee Member for various international conferences, such as IEEE PIMRC from 2013 to 2019, IEEE WCNC from 2014 to 2018, and IEEE VTC from 2015 to 2018. He currently serves as an Area Editor for the *Physical Communications* Journal (Elsevier), *Information* Journal (MDPI), *Sensors* (MDPI), and *Internet of Technology Letters* (Wiley). He also serves on the Advisory Board for *Journal of Multidisciplinary Sciences* (MDPI). He serves as a reviewer for various IEEE Transactions and other journals.